Supplementary

Crystal structure and XPS study of titanium-substituted M-type hexaferrite $BaFe_{12-x}Ti_xO_{19}$

MDPI Inorganics

Contents

1 WDS data and SEM patterns

The nominal and with WDS determined degrees of substitution, composition according to SCXRD and WDS measurement results for the five single crystals measured with WDS, XPS and some with SCXRD are listed in Table S1.

From twelve synthesized samples with different nominal degree of substitution x_{nom} several single crystals were selected and measured with WDS. For each sample, an arithmetic average $\bar{x}_{\mathrm{WDS}}$ was calculated from the obtained degrees of substitution from the individual crystals x_{WDS}. For all samples PXRD patterns were measured. Le Bail fits resulted in unit cell parameters a and c, and the cell volume V. These patterns including the Le Bail fits are shown in section PXRD diffractograms. Finally, a, c, and V are plotted against the arithmetic average substitution parameter $\bar{x}_{\mathrm{WDS}}$.

In Table S2 the WDS measurement results are listed with the nominal degrees of substitution x_{nom}, from WDS measurement x_{WDS} and average over all WDS measurements $\bar{x}_{\mathrm{WDS}}$ for crystals selected from the same sample.

The nominal degree of substitution x_{nom} was compared and discussed with the measured degree of substitution x_{WDS}. Degrees of substitution from Table S2 were taken and additionally a few more crystals were measured with WDS. The data for the additionally measured crystals are listed in Table S3.

Regarding the WDS measurements, the sum of all measured mass fractions should ideally amount to 100%. The observed small discrepancies (with ca. $\pm 3\%$) can have different reasons: Further elements could be contained in the compound, which is unlikely, as according to WDS all used starting materials are part of the product. Only small surface contaminations from side products, e.g. $BaTiO_3$, $NaFeTiO_4$ and $FeTiO_3$, were detected. Residue grease from preceding SCXRD measurements can still stick to the crystals surface and worsen the data. Most likely, the observed small loss of intensity is due to an inhomogeneous surface texture and slight tilting of the surface in relation to the electron beam.

1 WDS data and SEM patterns

Table S1: Nominal degree of substitution x_{nom} and from WDS measurements x_{WDS}, compositions according to SCXRD measurements and from WDS measurements obtained average mass fractions $\bar{\omega}$ for elements barium, iron, titanium, sodium and gold are listed. The mass fraction for oxygen is calculated assuming Ba^{2+}, Fe^{3+}, Ti^{4+}, Na^+, Au and O^{2-} and the total percentage is calculated, both are listed as well.

x_{nom}	composition SCXRD	x_{WDS}	$\bar{\omega}_{Ba}$ / %	$\bar{\omega}_{Fe}$ / %	$\bar{\omega}_{Ti}$ / %	$\bar{\omega}_{Na}$ / %	$\bar{\omega}_{Au}$ / %	$\bar{\omega}_{O}$ / %	**total** / %
0.0	unsubstituted ferrite	0	12.2(2)	59.1(9)	0	—	—	26.9	98.2
0.1	—	0.143(5)	12.5(2)	60.0(9)	0.63(2)	—	—	27.6	100.7
0.5	—	0.49(1)	11.4(2)	56.5(9)	2.07(4)	—	—	27.0	96.9
1.5	$BaFe_{11.3(2)}Ti_{0.7(2)}O_{19}$	0.62(1)	12.9(2)	55.7(12)	2.76(13)	0.63(7)	—	27.5	99.6
3.6	$BaFe_{8.8(4)}Ti_{3.2(4)}O_{19}$	0.91(7)	12.5(2)	50.5(9)	3.66(27)	0.50(7)	2.9(4)	25.8	98.9

Table S2: The nominal degrees of substitution x_{nom}, from WDS measurements x_{WDS} and average over all WDS measurements $\bar{x}_{WDS}$ for crystals selected from the same sample with a PXRD measurement. Average mass fractions $\bar{\omega}$ for elements barium, iron and titanium are listed. The mass fraction for oxygen is calculated assuming Ba^{2+}, Fe^{3+}, Ti^{4+} and O^{2-} and the total percentage is calculated, both are listed as well.

x_{nom}	x_{WDS}	$\bar{x}_{WDS}$	$\bar{\omega}_{Ba}$	$\bar{\omega}_{Fe}$	$\bar{\omega}_{Ti}$	$\bar{\omega}_O$	total
0.10	0.078(5)		12.4(2)	60.9(9)	0.34(2)	27.8	101.5
0.10	0.143(5)	0.12	12.5(2)	60.0(9)	0.63(2)	27.6	100.7
0.10	0.146(5)		12.8(2)	60.3(9)	0.64(2)	27.8	101.5
0.20	0.23(1)		12.6(2)	59.9(9)	1.00(3)	27.9	101.4
0.20	0.25(1)	0.25	12.6(2)	60.3(9)	1.12(3)	28.1	102.1
0.20	0.27(1)		12.5(2)	60.1(9)	1.21(3)	28.1	102.0
0.65	0.30(1)	0.30	12.7(2)	58.7(9)	1.31(3)	27.6	100.2
0.35	0.29(1)		12.8(2)	60.7(9)	1.28(3)	28.4	103.2
0.35	0.34(1)	0.37	12.4(2)	57.3(9)	1.45(3)	27.0	98.2
0.35	0.50(1)		13.3(2)	56.8(9)	2.14(4)	27.4	99.6
0.50	0.39(1)	0.39	12.6(2)	59.4(9)	1.71(3)	28.1	101.8
0.80	0.33(1)		12.6(2)	59.0(9)	1.45(3)	27.8	100.9
0.80	0.46(1)	0.42	12.5(2)	58.9(9)	2.04(3)	28.1	101.6
0.80	0.47(1)		12.5(2)	58.6(9)	2.07(3)	28.0	101.3
0.70	0.37(1)		12.7(2)	60.6(9)	1.65(3)	28.6	103.6
0.70	0.43(1)	0.43	12.6(2)	60.2(9)	1.95(3)	28.6	103.4
0.70	0.49(1)		12.7(2)	59.3(9)	2.21(4)	28.5	102.7
0.80	0.45(1)		13.2(2)	58.2(9)	1.99(3)	27.9	101.2
0.80	0.46(1)	0.46	13.0(2)	57.9(9)	2.01(3)	27.7	100.6
0.90	0.43(1)		12.6(2)	57.5(9)	1.85(3)	27.4	99.4
0.90	0.51(1)	0.48	12.6(2)	57.6(9)	2.22(4)	27.7	100.1
1.50	0.62(1)	0.62	12.2(2)	55.7(9)	2.64(4)	27.1	97.7
2.50	0.70(1)	0.70	12.2(2)	55.2(9)	2.98(4)	27.1	97.5

Table S3: Nominal degree of substitution $x_{\mathbf{nom}}$ and from WDS measurements x_{WDS}, average mass fractions $\bar{\omega}$ for elements barium, iron, titanium, sodium and gold are listed. The mass fraction for oxygen is calculated assuming Ba^{2+}, Fe^{3+}, Ti^{4+}, Na^+, Au and O^{2-} and the total percentage is calculated, both are listed as well.

$x_{\mathbf{nom}}$	$x_{\mathbf{WDS}}$	$\bar{\omega}_{\mathbf{Ba}}$ / %	$\bar{\omega}_{\mathbf{Fe}}$ / %	$\bar{\omega}_{\mathbf{Ti}}$ / %	$\bar{\omega}_{\mathbf{O}}$ / %	$\bar{\omega}_{\mathbf{Na}}$ / %	$\bar{\omega}_{\mathbf{Au}}$ / %	**total** / %
0.50	0.31(2)	12.5(2)	58.8(12)	1.34(9)	27.7	0.32(5)	–	100.6
0.65	0.32(2)	12.3(2)	55.7(12)	1.33(9)	26.3	0.24(5)	2.8(4)	98.6
0.35	0.35(4)	12.5(2)	53.0(9)	1.37(16)	25.3	0.38(6)	2.7(4)	95.2
1.20	0.44(2)	12.2(2)	56.3(12)	1.85(11)	27.0	0.23(5)	2.8(4)	100.4
1.00	0.45(3)	12.2(2)	55.5(12)	1.87(11)	26.6	0.24(5)	2.9(4)	99.4
1.10	0.51(3)	12.3(2)	56.2(12)	2.15(11)	27.1	0.34(6)	2.7(4)	100.9
0.90	0.58(3)	11.8(2)	56.8(12)	2.49(12)	27.5	0.26(5)	2.8(4)	101.6
0.80	0.61(3)	12.6(2)	54.7(11)	2.57(12)	26.9	0.58(7)	2.8(4)	100.2
0.70	0.65(3)	12.9(2)	55.7(12)	2.76(13)	27.5	0.63(7)	–	99.6
3.60	0.91(7)	12.5(2)	50.5(9)	3.66(27)	25.8	0.50(7)	2.9(4)	95.9

1 WDS data and SEM patterns

(a)   (b)
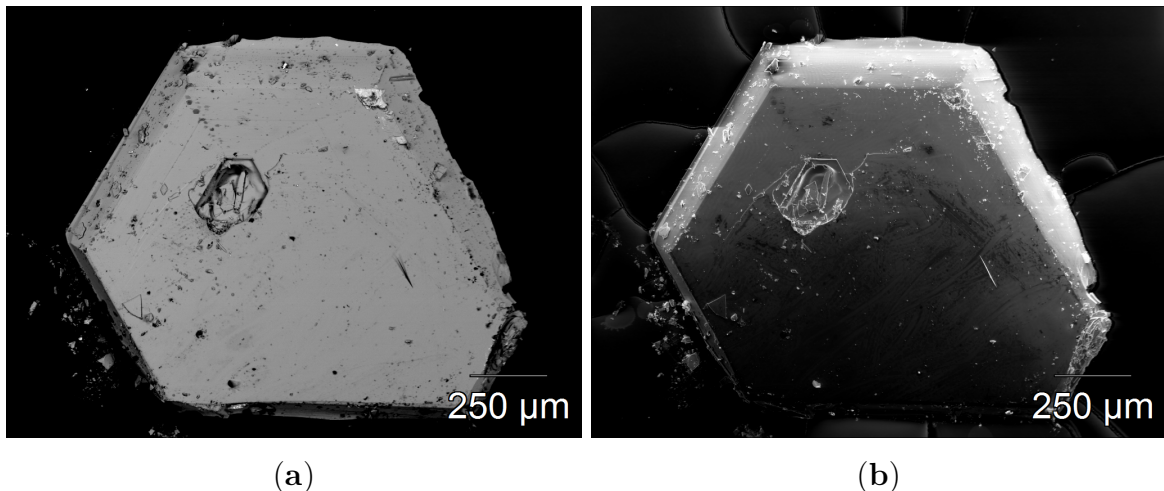
Figure S1: SEM pictures of substituted ferrite, $x = 0.078(5)$ **a**) BSE image **b**) SE image.

(a)   (b)
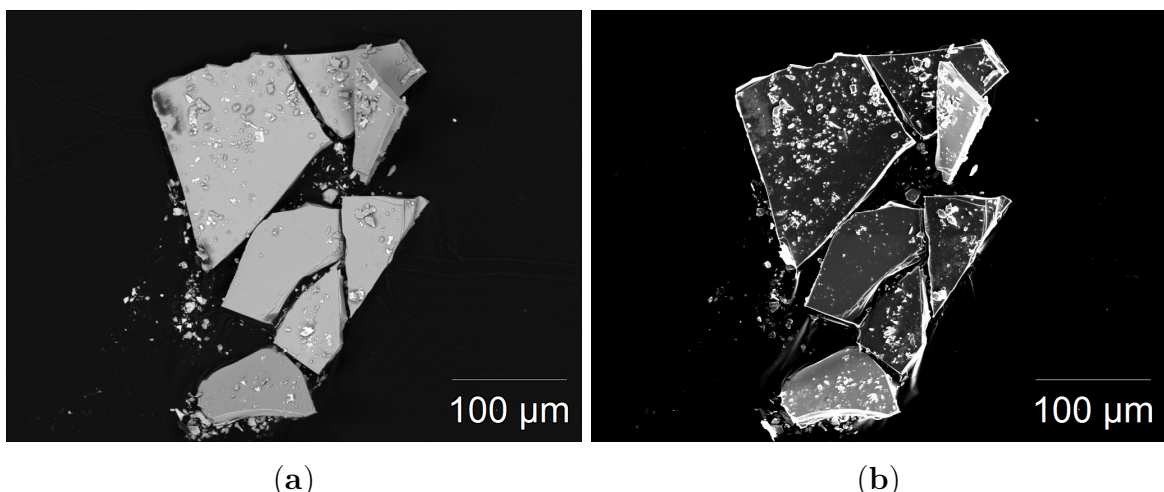
Figure S2: SEM pictures of substituted ferrite, $x = 0.31(2)$ **a**) BSE image **b**) SE image.


(a)   (b)
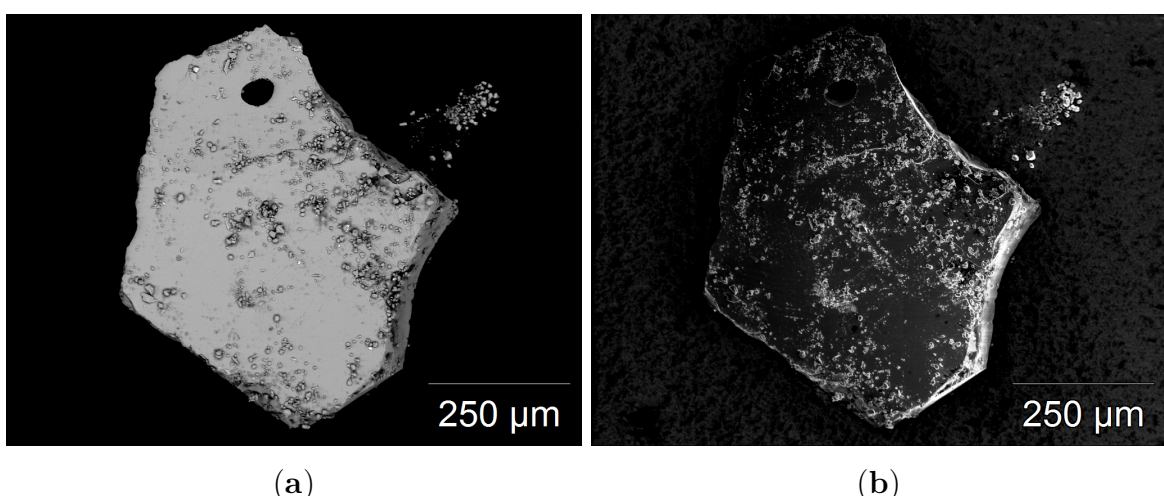
Figure S3: SEM pictures of substituted ferrite, $x = 0.44(2)$ **a**) BSE image **b**) SE image.

1 WDS data and SEM patterns

| (a) | (b) |
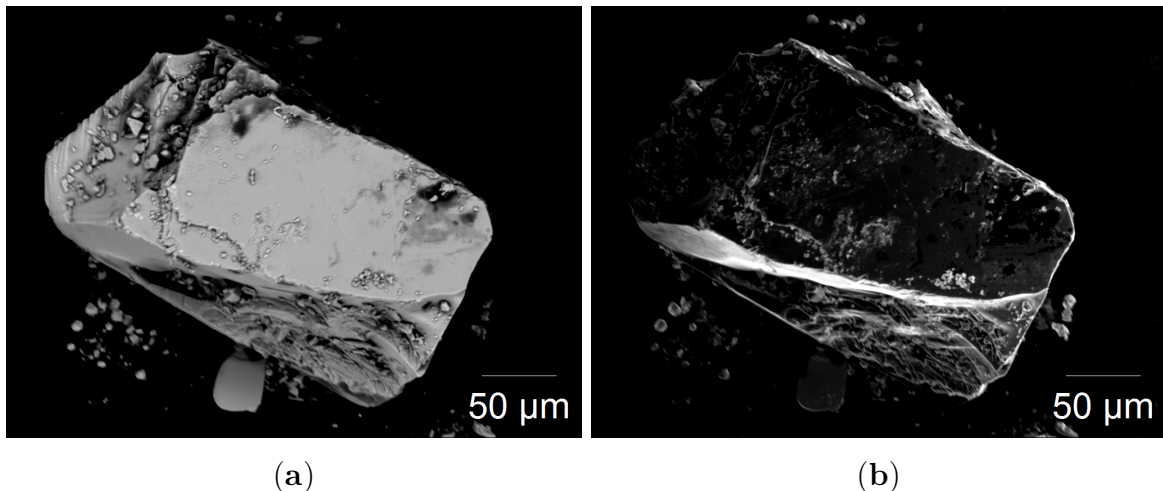
Figure S4: SEM pictures of substituted ferrite, $x = 0.45(3)$ **a**) BSE image **b**) SE image.

| (a) | (b) |
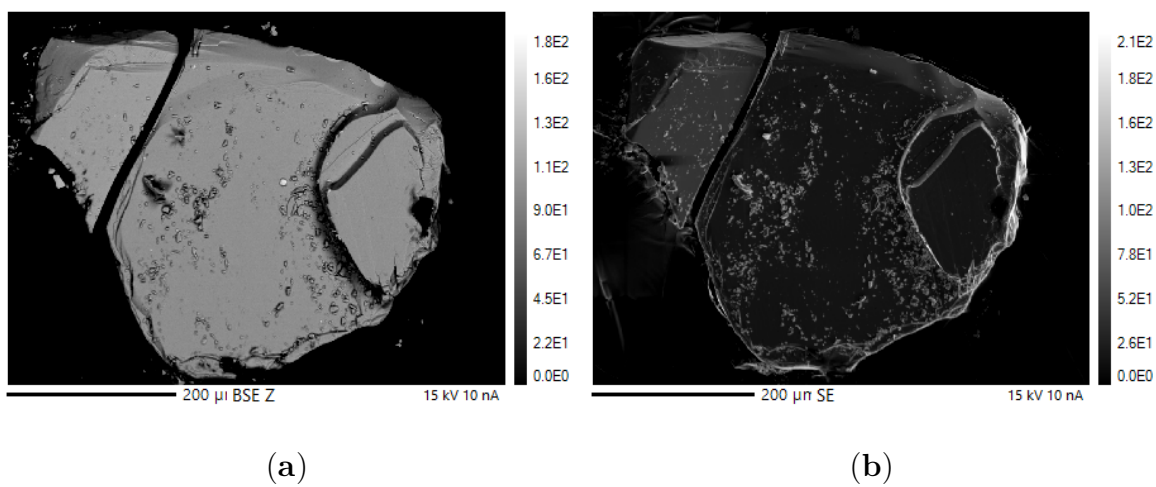
Figure S5: SEM pictures of substituted ferrite, $x = 0.49(1)$, measured with XPS as well, **a**) BSE image **b**) SE image.

| (a) | (b) |
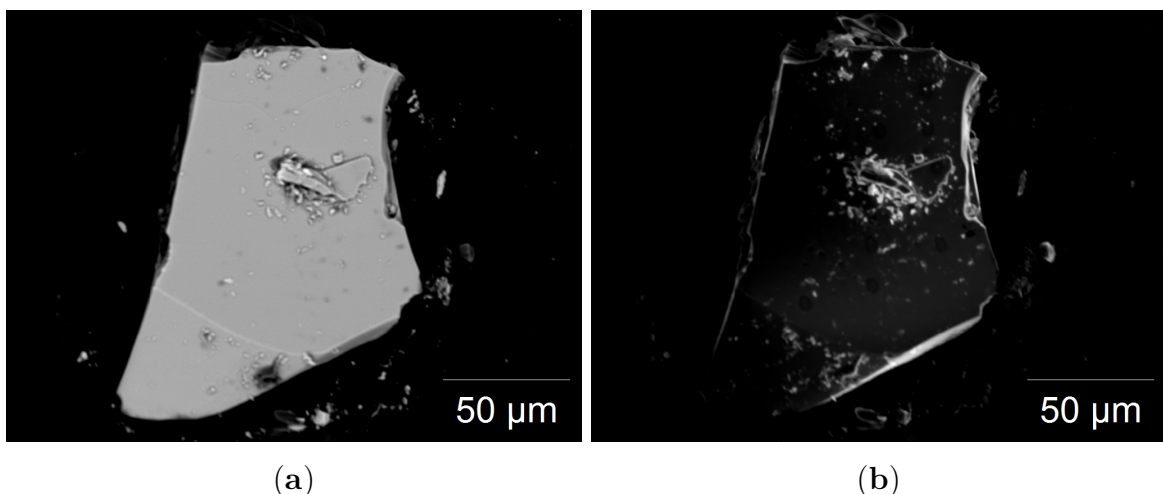
Figure S6: SEM pictures of substituted ferrite, $x = 0.58(3)$ **a**) BSE image **b**) SE image.

1 WDS data and SEM patterns

(**a**) (**b**)
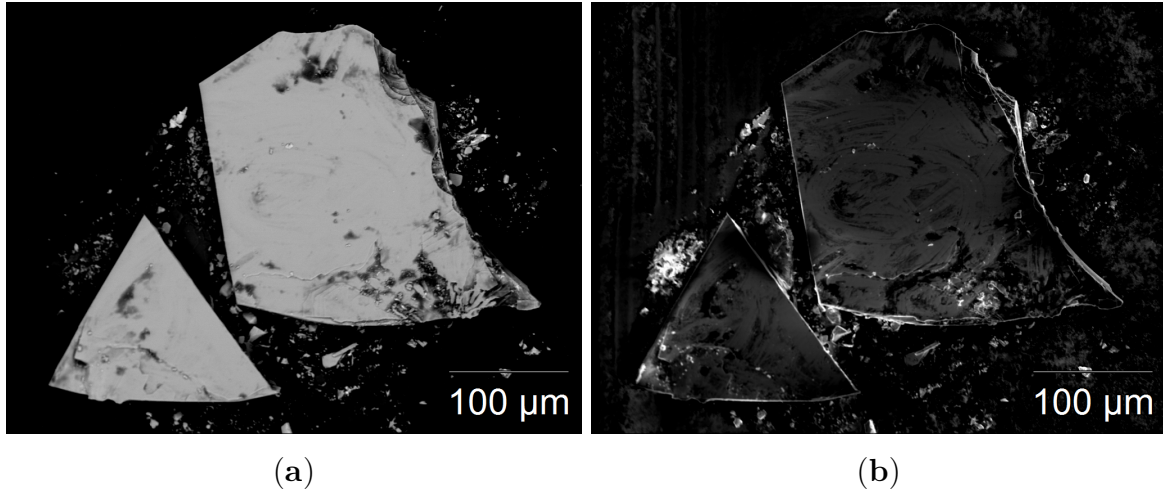
Figure S7: SEM pictures of substituted ferrite, $x = 0.61(3)$ **a**) BSE image **b**) SE image.

(**a**) (**b**)
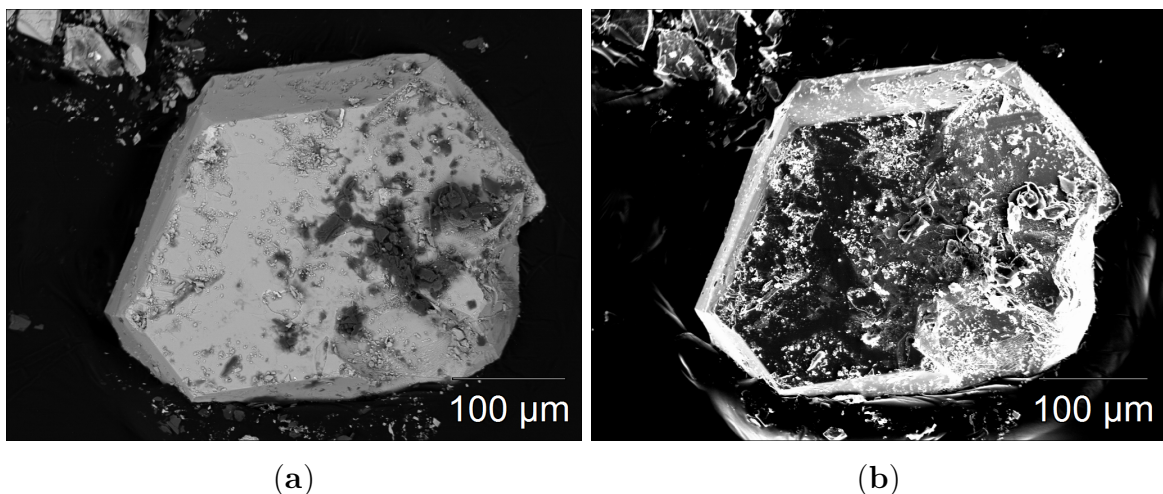
Figure S8: SEM pictures of substituted ferrite, $x = 0.65(3)$ **a**) BSE image **b**) SE image.

(**a**) (**b**)
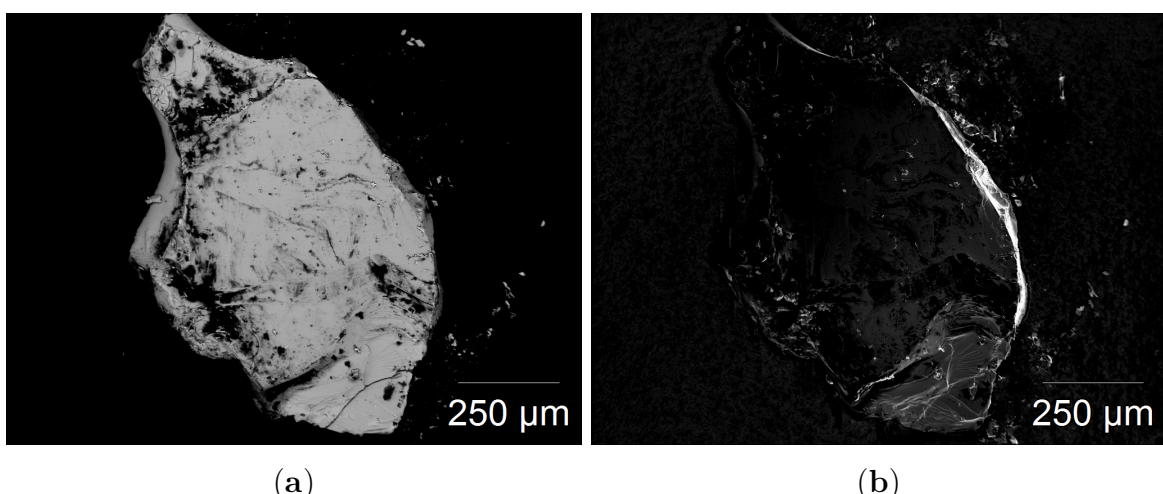
Figure S9: SEM pictures of substituted ferrite, $x = 0.91(7)$, measured with XPS as well, **a**) BSE image **b**) SE image.

2 SCXRD data

Table S4: Crystallographic data, device parameters and SCXRD refinement data for BaFe$_{12}$O$_{19}$.

crystal system	hexagonal
space group type	$P6_3/mmc$ (No. 194)
formula units per unit cell Z	2
a / pm	589.35(1)
c / pm	2319.62(5)
V / 10^6 pm^3	697.74(4)
calculated density D_x/ g $\cdot$ cm^{-3}	5.29
measuring device	κ-CCD (Bruker-Nonius)
λ / pm	71.07 (Mo-K_α)
$2\theta_{\max}$/ $^\circ$	54.94
$h/k/l$	$\pm 7/\pm 7/-29 \leq l \leq 30$
μ/ mm^{-1}	14.95
measured / unique reflections	10118 / 360
number of refined parameters	43
$R_{\mathrm{int}}/R_\sigma$	0.047 / 0.014
R_1/R_1 with $|F_\mathrm{o}| \geq 4\sigma(F_\mathrm{o})$	0.020 / 0.018
$wR_2/GooF$	0.052 / 1.408
max./min. $\rho(\mathrm{e}^-)$ / 10^{-6} pm^{-3}	0.43 / -0.63

Table S5: Wyckoff sites, fractional coordinates in the asymmetric unit and isotropic displacement parameters for each unique site in $BaFe_{12}O_{19}$.

Ion	Wyckoff site	$x\ /\ a$	$y\ /\ b$	$z\ /\ c$	$U_{\text{iso}}\ /\ \text{pm}^2$
Ba	$2d$	2/3	1/3	1/4	87(2)
$Fe_{VI}(1)$	$2a$	0	0	0	66(4)
$Fe_V(2)^a$	$4e$	0	0	0.2425(4)	67(15)
$Fe_{IV}(3)$	$4f$	1/3	2/3	0.02733(4)	63(3)
$Fe_{VI}(4)$	$4f$	1/3	2/3	0.19032(5)	64(3)
$Fe_{VI}(5)$	$12k$	0.3373(1)	$x/2$	0.10826(2)	67(2)
O(1)	$4e$	0	0	0.1503(2)	70(10)
O(2)	$4f$	2/3	1/3	0.0547(2)	81(11)
O(3)	$6h$	0.1815(4)	$2x$	1/4	82(9)
O(4)	$12k$	0.1565(3)	$2x$	0.0518(1)	68(6)
O(5)	$12k$	0.5023(3)	$\bar{x}$	0.1492(1)	75(6)

[a] occupation factor fixed to 50 %.

Table S6: Anisotropic displacement parameters for each site in $BaFe_{12}O_{19}$.

Ion	$U_{11}\ /\ \text{pm}^2$	$U_{22}\ /\ \text{pm}^2$	$U_{33}\ /\ \text{pm}^2$	$U_{23}\ /\ \text{pm}^2$	$U_{13}\ /\ \text{pm}^2$	$U_{12}\ /\ \text{pm}^2$
Ba	92(3)	U_{11}	79(4)	0	0	$U_{11}/2$
$Fe_{VI}(1)$	73(5)	U_{11}	54(7)	0	0	$U_{11}/2$
$Fe_V(2)$	60(5)	U_{11}	82(46)	0	0	$U_{11}/2$
$Fe_{IV}(3)$	64(4)	U_{11}	60(5)	0	0	$U_{11}/2$
$Fe_{VI}(4)$	69(4)	U_{11}	53(5)	0	0	$U_{11}/2$
$Fe_{VI}(5)$	64(4)	69(3)	67(4)	−3(1)	$2U_{23}$	$U_{11}/2$
O(1)	80(16)	U_{11}	52(23)	0	0	$U_{11}/2$
O(2)	97(16)	U_{11}	48(24)	0	0	$U_{11}/2$
O(3)	103(16)	72(22)	60(20)	0	0	$U_{22}/2$
O(4)	79(11)	69(15)	53(14)	14(11)	$U_{23}/2$	$U_{22}/2$
O(5)	76(11)	U_{11}	61(14)	6(6)	$−U_{23}$	75(6)

2 SCXRD data

Table S7: Crystallographic data, device parameters and SCXRD refinement data for $BaFe_{11.1(2)}Ti_{0.65(3)}\square_{0.25}O_{19}$.

composition from XRD	$BaFe_{11.3(2)}Ti_{0.7(2)}O_{19}$
crystal system	hexagonal
space group type	$P6_3/mmc$ (No. 194)
formula units per unit cell Z	2
a / pm	590.72(6)
c / pm	2339.5(4)
V / 10^6 pm^3	707.0(3)
calculated density D_x/ g $\cdot$ cm^{-3}	5.20
measuring device	IPDS-I (STOE)
λ / pm	71.07 (Mo-K_α)
$2\theta_{max}$/ $^\circ$	59.80
$h/k/l$	$\pm7/\pm8/\pm32$
μ/ mm^{-1}	14.45
measured / unique reflections	7538 / 451
number of refined parameters	46
R_{int}/R_σ	0.053 / 0.019
R_1/R_1 with $|F_o| \geq 4\sigma(F_o)$	0.039 / 0.027
$wR_2/GooF$	0.065 / 1.033
max./min. $\rho(e^-)$ / 10^{-6} pm^{-3}	0.90 / -1.59

Table S8: Wyckoff sites, fractional coordinates in the asymmetric unit, occupation factor and isotropic displacement parameters for each unique site in $BaFe_{11.1(2)}Ti_{0.65(3)}\square_{0.25}O_{19}$. Sites M are mixed occupied by Fe and Ti.

Ion	Wyckoff site	x / a	y / b	z / c	occupation Fe/Ti / %	U_{iso} / pm^2
Ba	$2d$	2/3	1/3	1/4	–	61(2)
Fe$_{\mathrm{VI}}$(1)	$2a$	0	0	0	–	40(3)
Fe$_{\mathrm{V}}$(2)[a]	$4e$	0	0	0.2427(4)	–	72(15)
M_{IV}(3)	$4f$	1/3	2/3	0.02703(4)	89/11(3)	37(4)
M_{VI}(4)	$4f$	1/3	2/3	0.18991(4)	87/13(3)	36(3)
M_{VI}(5)	$12k$	0.3368(1)	$x/2$	0.10815(3)	97/3(2)	35(2)
O(1)	$4e$	0	0	0.1514(2)	–	44(9)
O(2)	$4f$	2/3	1/3	0.0557(2)	–	47(10)
O(3)	$6h$	0.1820(4)	$2x$	1/4	–	48(8)
O(4)	$12k$	0.1561(3)	$2x$	0.0522(1)	–	51(6)
O(5)	$12k$	0.5017(3)	$\bar{x}$	0.1497(1)	–	41(6)

[a] occupation factor fixed to 50 %.

Table S9: Anisotropic displacement parameters for each site in $BaFe_{11.1(2)}Ti_{0.65(3)}\square_{0.25}O_{19}$.

Ion	U_{11} / pm^2	U_{22} / pm^2	U_{33} / pm^2	U_{23} / pm^2	U_{13} / pm^2	U_{12} / pm^2
Ba	62(2)	U_{11}	60(3)	0	0	$U_{11}/2$
Fe$_{\mathrm{VI}}$(1)	40(4)	U_{11}	39(6)	0	0	$U_{11}/2$
Fe$_{\mathrm{V}}$(2)	17(5)	U_{11}	182(47)	0	0	$U_{11}/2$
M_{IV}(3)	32(4)	U_{11}	46(5)	0	0	$U_{11}/2$
M_{VI}(4)	33(4)	U_{11}	40(5)	0	0	$U_{11}/2$
M_{VI}(5)	27(3)	35(3)	42(3)	−1(1)	$2U_{23}$	$U_{11}/2$
O(1)	36(14)	U_{11}	59(21)	0	0	$U_{11}/2$
O(2)	34(14)	U_{11}	73(23)	0	0	$U_{11}/2$
O(3)	52(14)	27(19)	55(19)	0	0	$U_{22}/2$
O(4)	53(11)	58(14)	43(14)	−17(12)	$U_{23}/2$	$U_{22}/2$
O(5)	32(10)	U_{11}	50(13)	−13(6)	$−U_{23}$	10(10)

Table S10: Crystallographic data, device parameters and SCXRD refinement data for $BaFe_{10.7(2)}Ti_{0.91(7)}\square_{0.36}O_{19}$.

composition from XRD	$BaFe_{9.0(4)}Ti_{3.0(4)}O_{19}$
crystal system	hexagonal
space group type	$P6_3/mmc$ (No. 194)
formula units per unit cell Z	2
a / pm	589.57(2)
c / pm	2324.8(1)
V / 10^6 pm^3	699.82(9)
calculated density D_x/ g $\cdot$ cm^{-3}	5.16
measuring device	STADIVARI (STOE)
λ / pm	71.07 (Mo-K_α)
$2\theta_{max}$/ $^\circ$	65.80
$h/k/l$	$\pm 8/\pm 8/-35 \leq l \leq 33$
μ/ mm^{-1}	13.49
measured / unique reflections	4328 / 552
number of refined parameters	46
R_{int}/R_σ	0.091 / 0.052
R_1/R_1 with $|F_o| \geq 4\sigma(F_o)$	0.102 / 0.065
$wR_2/GooF$	0.189 / 1.072
max./min. ρ(e$^-$) / 10^{-6} pm^{-3}	4.38 / -2.77

Table S11: Wyckoff sites, fractional coordinates in the asymmetric unit, occupation factor and isotropic displacement parameters for each unique site in $BaFe_{10.7(2)}Ti_{0.91(7)}\square_{0.36}O_{19}$. Sites M are mixed occupied by Fe and Ti.

Ion	Wyckoff site	x / a	y / b	z / c	occupation Fe/Ti / %	U_{iso} / pm^2
Ba	$2d$	2/3	1/3	1/4	–	132(5)
$Fe_{VI}(1)$	$2a$	0	0	0	–	122(8)
$Fe_V(2)^a$	$4e$	0	0	0.2415(3)	–	122(18)
$M_{IV}(3)$	$4f$	1/3	2/3	0.0267(1)	83/17(6)	105(8)
$M_{VI}(4)$	$4f$	1/3	2/3	0.1898(1)	64/36(6)	96(7)
$M_{VI}(5)$	$12k$	0.3363(3)	$x/2$	0.10787(5)	67/33(3)	96(5)
O(1)	$4e$	0	0	0.1517(5)	–	165(26)
O(2)	$4f$	2/3	1/3	0.0555(5)	–	116(23)
O(3)	$6h$	0.1807(9)	$2x$	1/4	–	114(20)
O(4)	$12k$	0.1562(7)	$2x$	0.0519(3)	–	128(16)
O(5)	$12k$	0.5015(7)	$\bar{x}$	0.1495(3)	–	144(15)

^{a} occupation factor fixed to 50 %.

Table S12: Anisotropic displacement parameters for each site in $BaFe_{10.7(2)}Ti_{0.91(7)}\square_{0.36}O_{19}$.

Ion	U_{11} / pm^2	U_{22} / pm^2	U_{33} / pm^2	U_{23} / pm^2	U_{13} / pm^2	U_{12} / pm^2
Ba	152(6)	U_{11}	91(6)	0	0	$U_{11}/2$
$Fe_{VI}(1)$	146(11)	U_{11}	74(11)	0	0	$U_{11}/2$
$Fe_V(2)$	102(12)	U_{11}	160(56)	0	0	$U_{11}/2$
$M_{IV}(3)$	118(10)	U_{11}	80(11)	0	0	$U_{11}/2$
$M_{VI}(4)$	108(10)	U_{11}	72(10)	0	0	$U_{11}/2$
$M_{VI}(5)$	117(9)	109(7)	64(7)	0(3)	$2U_{23}$	$U_{11}/2$
O(1)	201(42)	U_{11}	93(40)	0	0	$U_{11}/2$
O(2)	146(37)	U_{11}	58(42)	0	0	$U_{11}/2$
O(3)	121(36)	148(52)	83(35)	0	0	$U_{22}/2$
O(4)	141(27)	155(38)	93(26)	−55(26)	$U_{23}/2$	$U_{22}/2$
O(5)	159(26)	U_{11}	84(23)	−13(13)	$−U_{23}$	58(30)

2 SCXRD data

Table S13: Crystallographic data, device parameters and SCXRD refinement data for $BaFe_{11.2(2)}Ti_{0.61(3)}\square_{0.24}O_{19}$.

composition from XRD	$BaFe_{10.7(3)}Ti_{1.3(3)}O_{19}$
crystal system	hexagonal
space group type	$P6_3/mmc$ (No. 194)
formula units per unit cell Z	2
a / pm	590.89(4)
c / pm	2332.2(2)
V / 10^6 pm^3	705.2(2)
calculated density D_x/ g $\cdot$ cm^{-3}	5.20
measuring device	IPDS-I (STOE)
λ / pm	71.07 (Mo-K_α)
$2\theta_{max}$/ $°$	59.85
$h/k/l$	$-7 \leq h \leq 8/ \pm 8/ \pm 32$
μ/ mm^{-1}	14.33
measured / unique reflections	7626 / 451
number of refined parameters	46
R_{int}/R_σ	0.073 / 0.025
R_1/R_1 with $|F_o| \geq 4\sigma(F_o)$	0.052 / 0.041
$wR_2/GooF$	0.094 / 1.225
max./min. $\rho(e^-)$ / 10^{-6} pm^{-3}	1.31 / -2.43

Table S14: Wyckoff sites, fractional coordinates in the asymmetric unit, occupation factor and isotropic displacement parameters for each unique site in $BaFe_{11.2(2)}Ti_{0.61(3)}\square_{0.24}O_{19}$. Sites M are mixed occupied by Fe and Ti.

Ion	Wyckoff site	x / a	y / b	z / c	occupation Fe/Ti / %	U_{iso} / pm^2
Ba	$2d$	2/3	1/3	1/4	–	65(5)
$Fe_{VI}(1)$	$2a$	0	0	0	–	44(4)
$Fe_V(2)^a$	$4e$	0	0	0.2431(7)	–	82(24)
$M_{IV}(3)$	$4f$	1/3	2/3	0.02702(6)	88/12(4)	40(5)
$M_{VI}(4)$	$4f$	1/3	2/3	0.18994(6)	81/19(4)	33(5)
$M_{VI}(5)$	$12k$	0.3370(2)	$x/2$	0.10816(4)	89/11(3)	30(3)
O(1)	$4e$	0	0	0.1516(2)	–	72(14)
O(2)	$4f$	2/3	1/3	0.0557(3)	–	50(13)
O(3)	$6h$	0.1822(6)	$2x$	1/4	–	39(12)
O(4)	$12k$	0.1562(4)	$2x$	0.0522(2)	–	51(9)
O(5)	$12k$	0.5014(4)	$\bar{x}$	0.1497(2)	–	39(9)

^{a} occupation factor fixed to 50 %.

Table S15: Anisotropic displacement parameters for each site in $BaFe_{11.2(2)}Ti_{0.61(3)}\square_{0.24}O_{19}$.

Ion	U_{11} / pm^2	U_{22} / pm^2	U_{33} / pm^2	U_{23} / pm^2	U_{13} / pm^2	U_{12} / pm^2
Ba	67(3)	U_{11}	60(4)	0	0	$U_{11}/2$
$Fe_{VI}(1)$	48(8)	U_{11}	36(9)	0	0	$U_{11}/2$
$Fe_V(2)$	17(7)	U_{11}	211(75)	0	0	$U_{11}/2$
$M_{IV}(3)$	36(6)	U_{11}	49(8)	0	0	$U_{11}/2$
$M_{VI}(4)$	33(5)	U_{11}	33(7)	0	0	$U_{11}/2$
$M_{VI}(5)$	22(5)	27(4)	40(5)	$-1(2)$	$2U_{23}$	$U_{11}/2$
O(1)	83(22)	U_{11}	48(28)	0	0	$U_{11}/2$
O(2)	48(20)	U_{11}	54(32)	0	0	$U_{11}/2$
O(3)	60(20)	35(27)	13(24)	0	0	$U_{22}/2$
O(4)	50(15)	69(20)	40(18)	$-22(16)$	$U_{23}/2$	$U_{22}/2$
O(5)	33(14)	U_{11}	44(17)	$-15(7)$	$-U_{23}$	11(15)

3 PXRD diffractograms
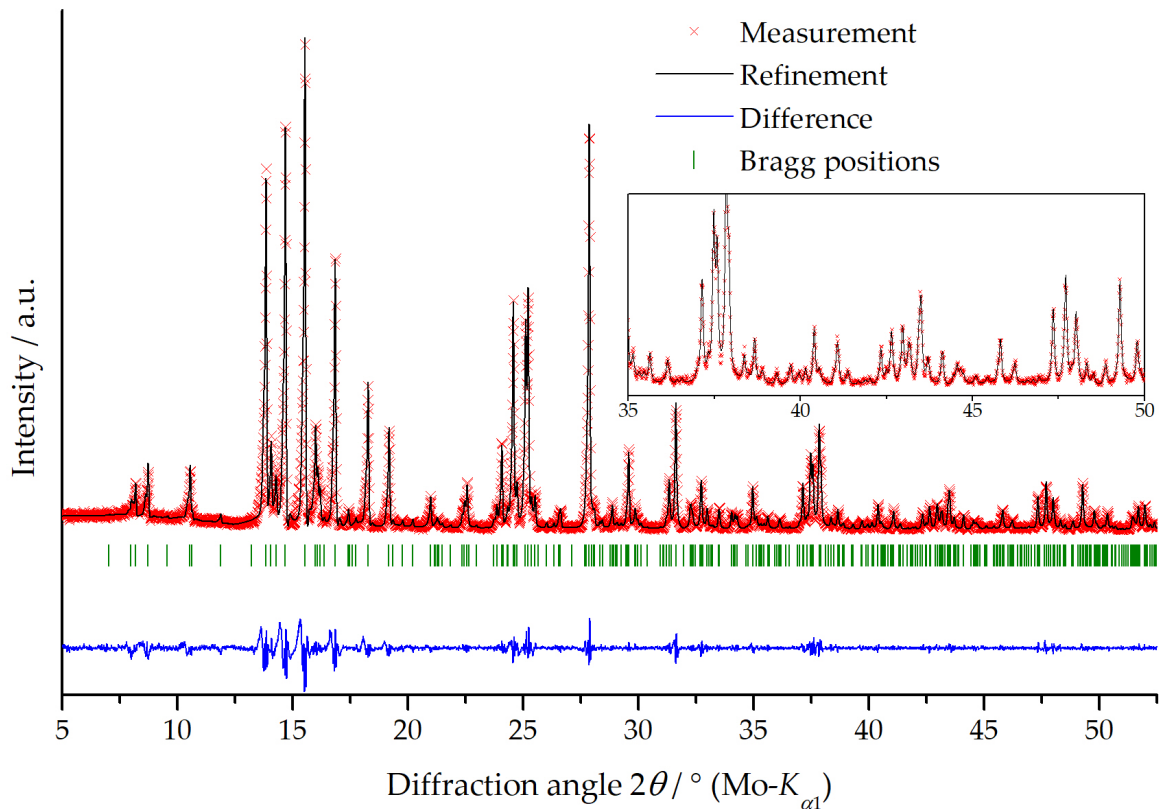
Figure S10: PXRD measurement (red) of nominal unsubstituted ferrite, $\bar{x}_{\mathrm{WDS}} = 0$, with Le Bail refinement (black) for calculating cell parameter a and c, difference (blue) and possible Bragg positions (green). Inset: enlargement of range between 35° and 50°.

Figure S11: PXRD measurement (red) of nominal $BaFe_{11.90}Ti_{0.10}O_{19}$, $\bar{x}_{WDS} = 0.12$, with Le Bail refinement (black) for calculating cell parameter a and c, difference (blue) and possible Bragg positions (green). Inset: enlargement of range between 35° and 50°.
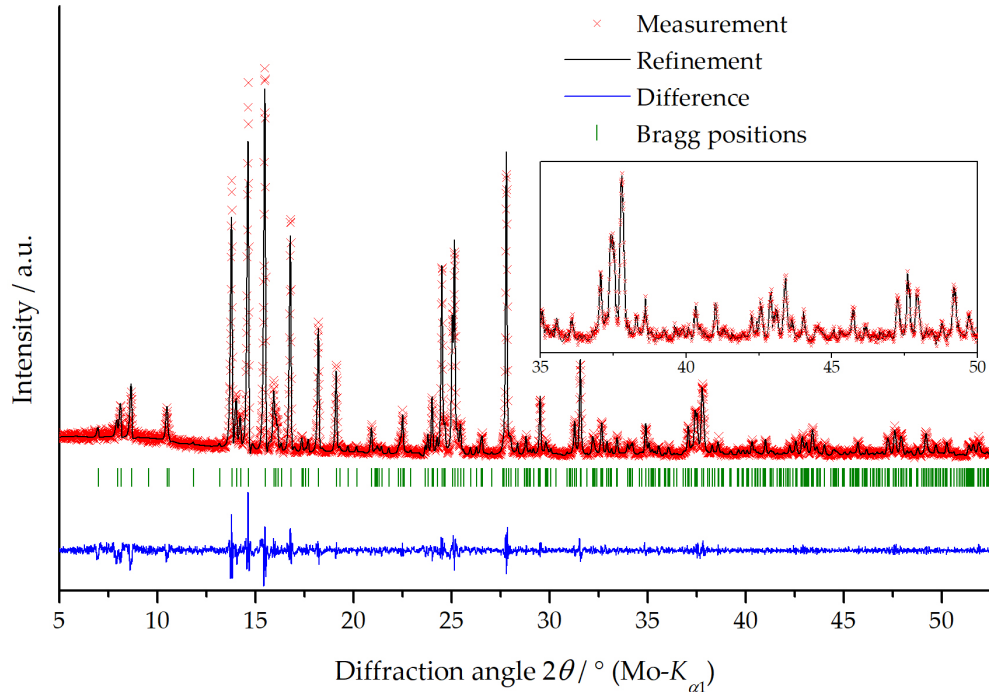
Figure S12: PXRD measurement (red) of nominal $BaFe_{11.80}Ti_{0.20}O_{19}$, $\bar{x}_{WDS} = 0.25$, with Le Bail refinement (black) for calculating cell parameter a and c, difference (blue) and possible Bragg positions (green). Inset: enlargement of range between 35° and 50°.

Figure S13: PXRD measurement (red) of nominal $BaFe_{11.35}Ti_{0.65}O_{19}$, $\bar{x}_{WDS} = 0.3$, with Le Bail refinement (black) for calculating cell parameter a and c, difference (blue) and possible Bragg positions (green). Inset: enlargement of range between 35° and 50°.
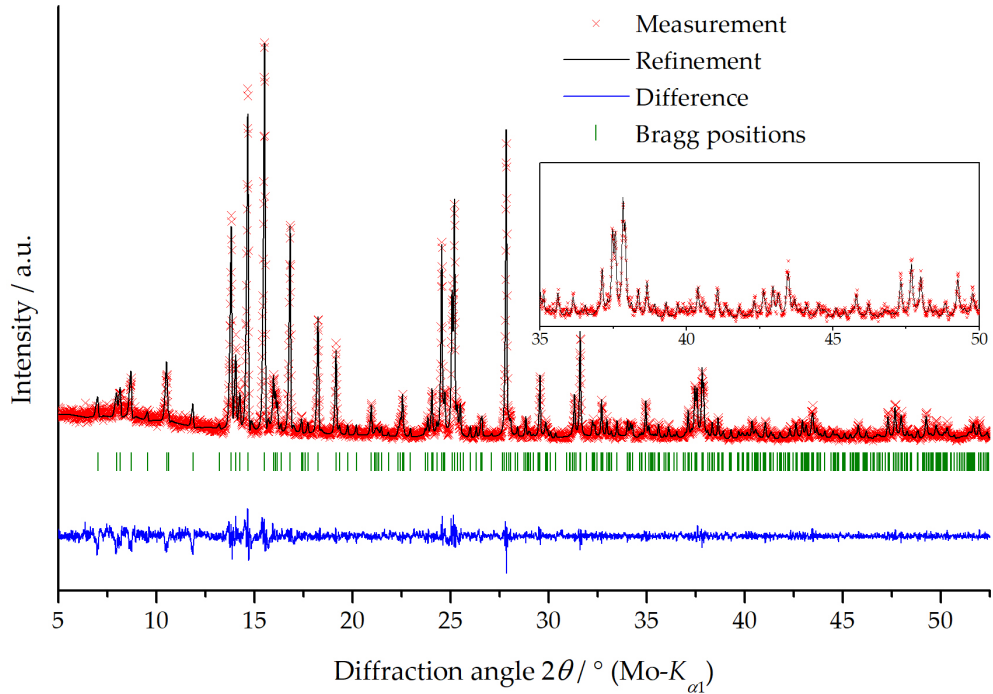
Figure S14: PXRD measurement (red) of nominal $BaFe_{11.65}Ti_{0.35}O_{19}$, $\bar{x}_{WDS} = 0.37$, with Le Bail refinement (black) for calculating cell parameter a and c, difference (blue) and possible Bragg positions (green). Inset: enlargement of range between 35° and 50°.

3 PXRD diffractograms
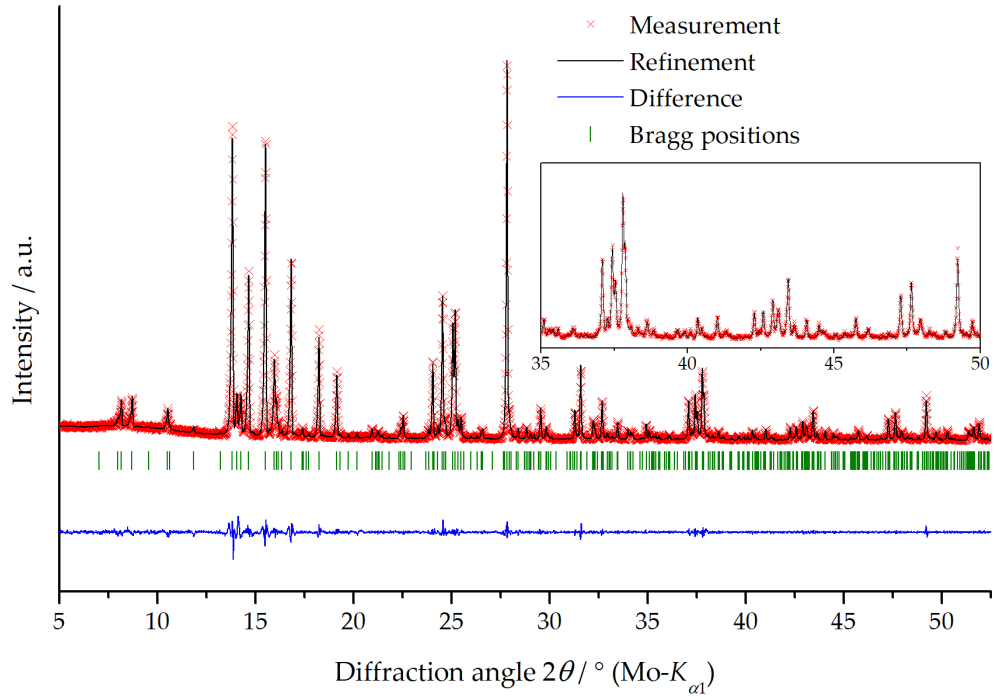
Figure S15: PXRD measurement (red) of nominal $BaFe_{11.50}Ti_{0.50}O_{19}$, $\bar{x}_{WDS} = 0.39$, with Le Bail refinement (black) for calculating cell parameter a and c, difference (blue) and possible Bragg positions (green). Inset: enlargement of range between $35°$ and $50°$.
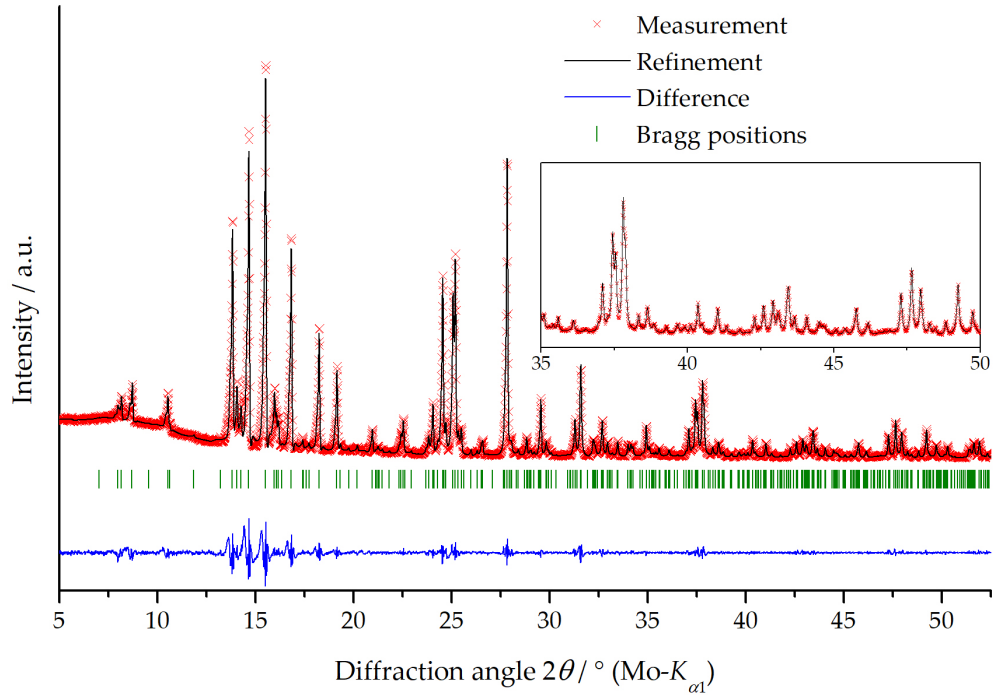
Figure S16: PXRD measurement (red) of nominal $BaFe_{11.20}Ti_{0.80}O_{19}$, $\bar{x}_{WDS} = 0.42$, with Le Bail refinement (black) for calculating cell parameter a and c, difference (blue) and possible Bragg positions (green). Inset: enlargement of range between $35°$ and $50°$.

Figure S17: PXRD measurement (red) of nominal $BaFe_{11.30}Ti_{0.70}O_{19}$, $\bar{x}_{WDS} = 0.43$, with Le Bail refinement (black) for calculating cell parameter a and c, difference (blue) and possible Bragg positions (green). Inset: enlargement of range between 35° and 50°.
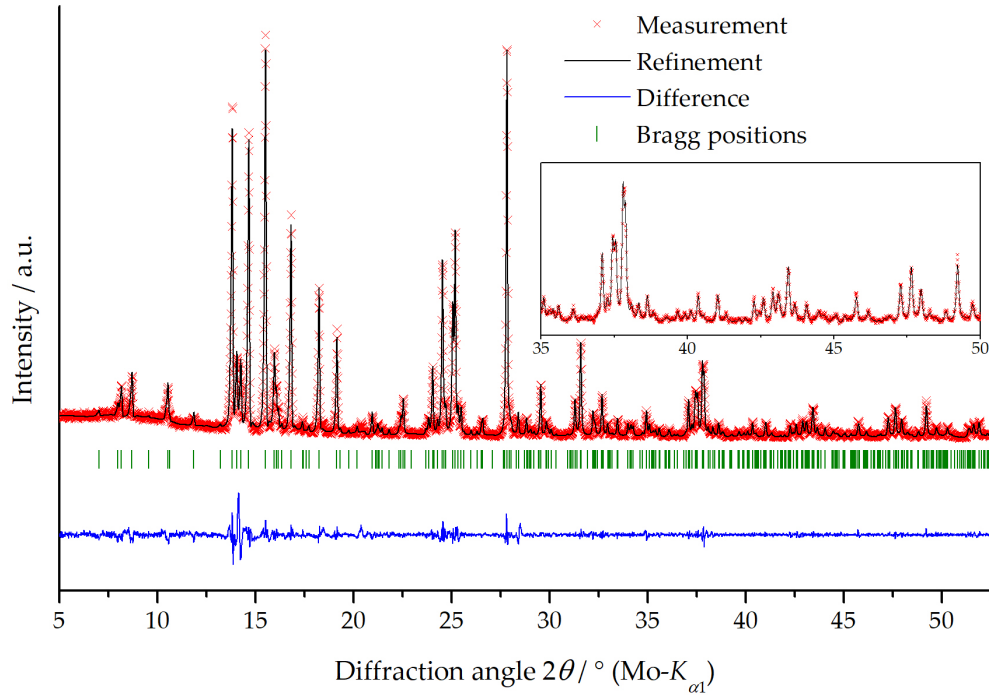
Figure S18: PXRD measurement (red) of nominal $BaFe_{11.20}Ti_{0.80}O_{19}$, $\bar{x}_{WDS} = 0.46$, with Le Bail refinement (black) for calculating cell parameter a and c, difference (blue) and possible Bragg positions (green). Inset: enlargement of range between 35° and 50°.

Figure S19: PXRD measurement (red) of nominal $BaFe_{11.10}Ti_{0.90}O_{19}$, $\bar{x}_{WDS} = 0.48$, with Le Bail refinement (black) for calculating cell parameter a and c, difference (blue) and possible Bragg positions (green). Inset: enlargement of range between 35° and 50°.
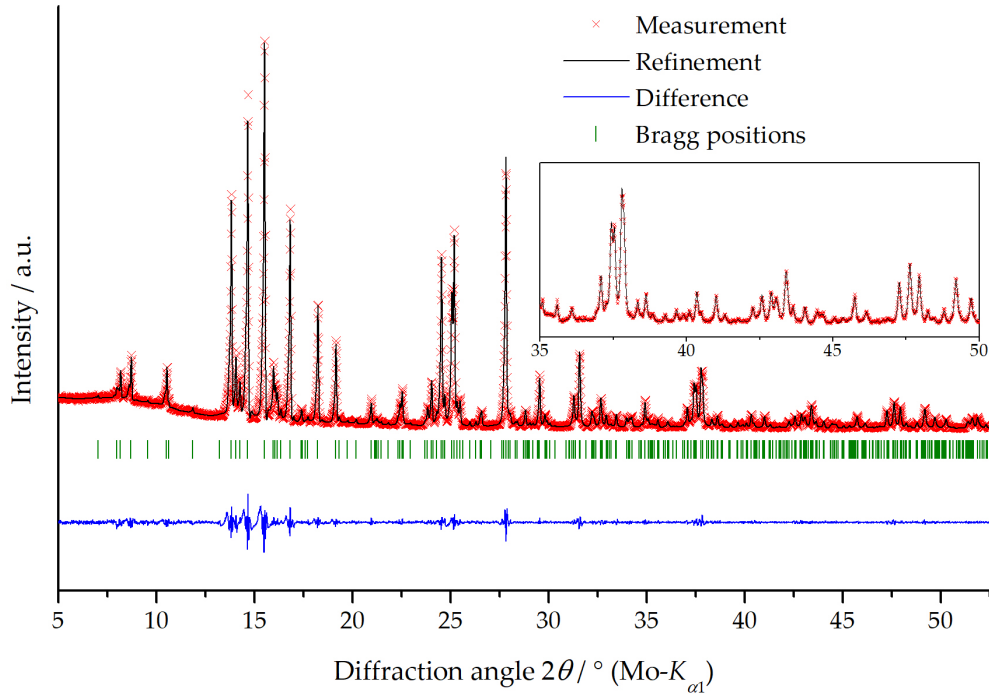
Figure S20: PXRD measurement (red) of nominal $BaFe_{10.50}Ti_{1.50}O_{19}$, $\bar{x}_{WDS} = 0.62$, with Le Bail refinement (black) for calculating cell parameter a and c, difference (blue) and possible Bragg positions (green). Inset: enlargement of range between 35° and 50°.

Figure S21: PXRD measurement (red) of nominal $BaFe_{9.50}Ti_{2.50}O_{19}$, $\bar{x}_{WDS} = 0.70$, with Le Bail refinement (black) for calculating cell parameter a and c, difference (blue) and possible Bragg positions (green). Inset: enlargement of range between 35° and 50°.

4 XPS data

4.1 XPS measurement spectra with pass energy 100 eV
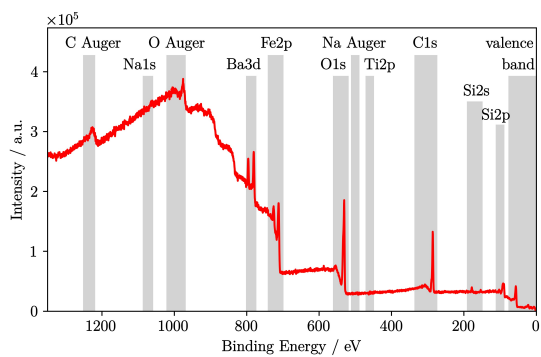
Figure S22: XPS survey spectrum of unsubstituted ferrite point 1.
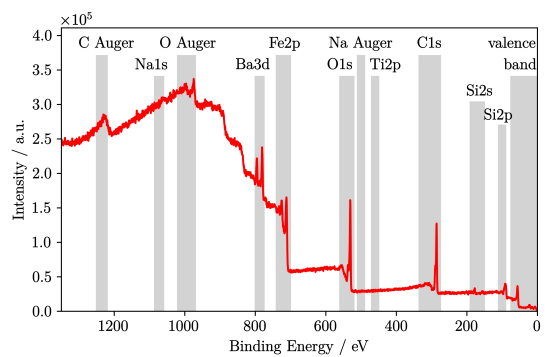
Figure S23: XPS survey spectrum of unsubstituted ferrite point 2.
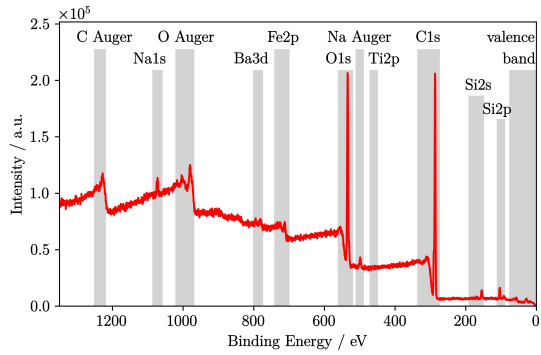
Figure S24: XPS survey spectrum of substituted ferrite, $x = 0.143(5)$ point 1.
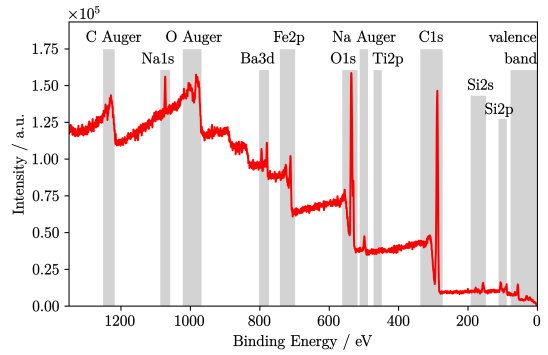
Figure S25: XPS survey spectrum of substituted ferrite, $x = 0.143(5)$ point 2.

4 XPS data
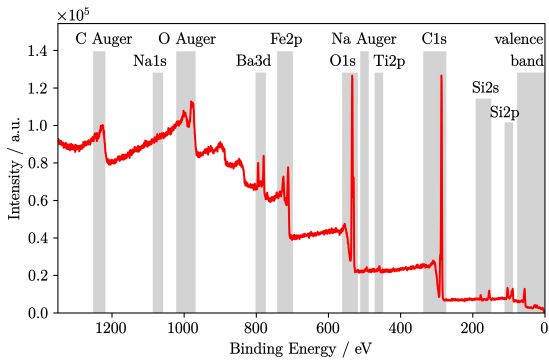
Figure S26: XPS survey spectrum of substituted ferrite, $x = 0.49(1)$ point 1.
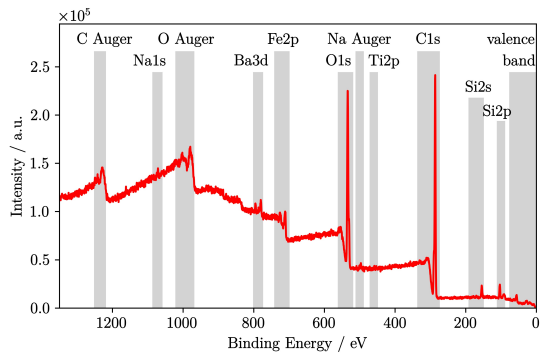
Figure S27: XPS survey spectrum of substituted ferrite, $x = 0.62(1)$ point 1.
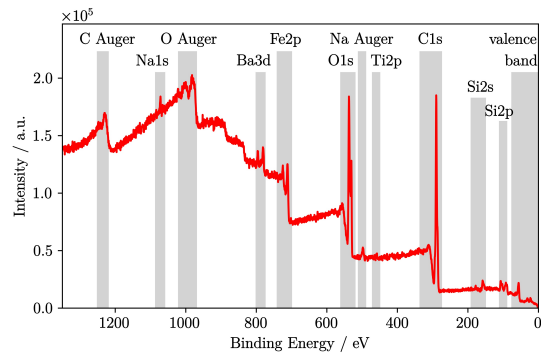
Figure S28: XPS survey spectrum of substituted ferrite, $x = 0.62(1)$ point 2.
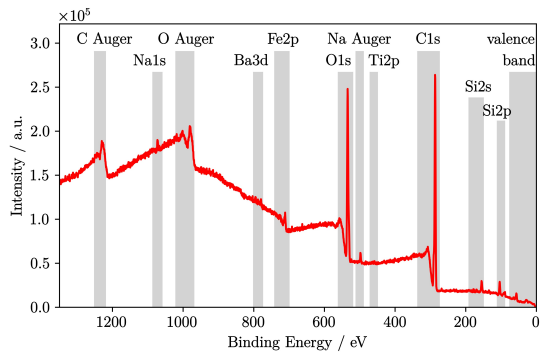
Figure S29: XPS survey spectrum of substituted ferrite, $x = 0.91(7)$ point 1.
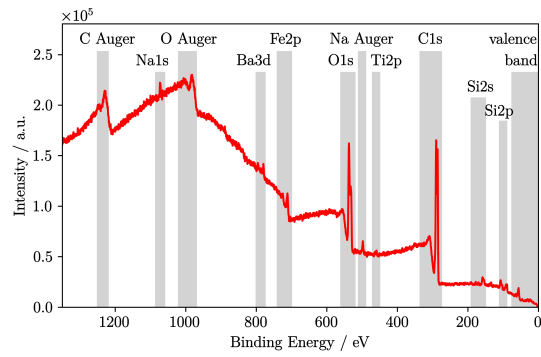
Figure S30: XPS survey spectrum of substituted ferrite, $x = 0.91(7)$ point 2.

4 XPS data
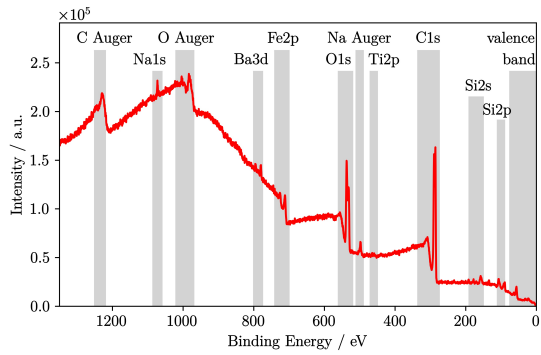
Figure S31: XPS survey spectrum of substituted ferrite, $x = 0.91(7)$ point 3.
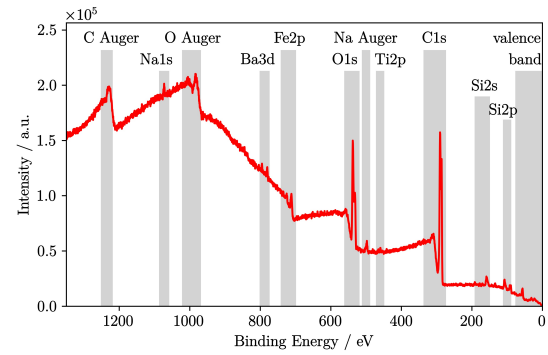
Figure S32: XPS survey spectrum of substituted ferrite, $x = 0.91(7)$ point 4.

4.2 XPS measurement spectra with pass energy 30 eV
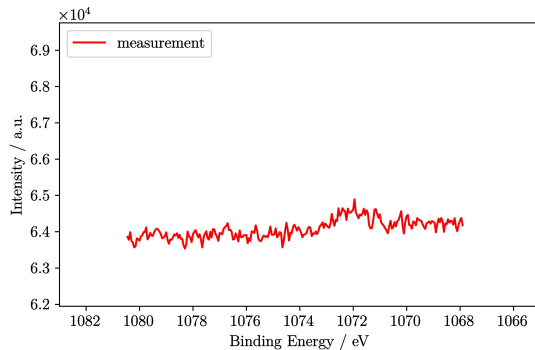
Figure S33: XPS Na 1s spectrum of unsubstituted ferrite point 1.
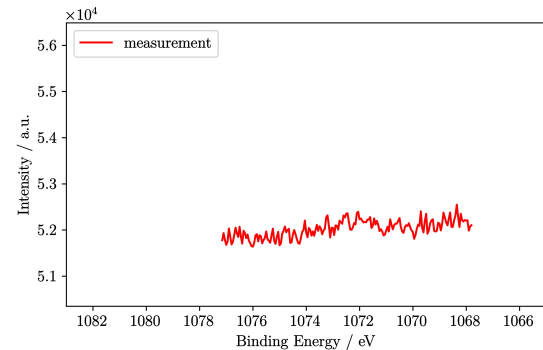
Figure S34: XPS Na 1s spectrum of unsubstituted ferrite point 2.
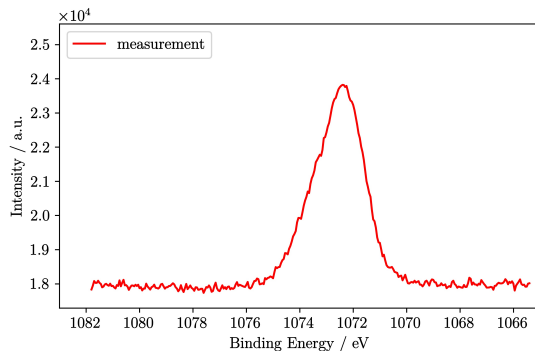
Figure S35: XPS Na 1s spectrum of substituted ferrite, $x = 0.143(5)$ point 1.
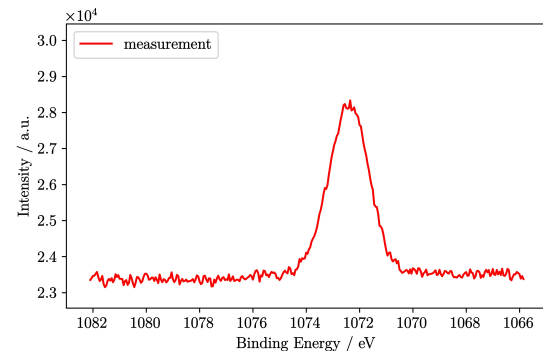
Figure S36: XPS Na 1s spectrum of substituted ferrite, $x = 0.143(5)$ point 2.
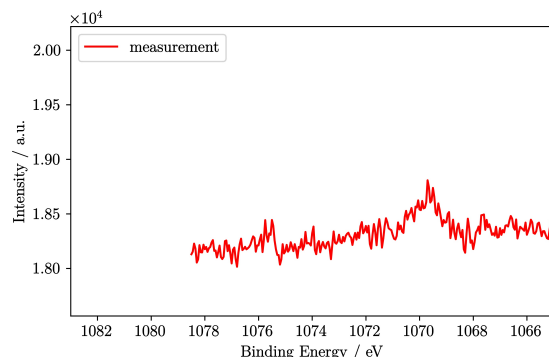
Figure S37: XPS Na 1s spectrum of substituted ferrite, $x = 0.49(1)$ point 1.

Figure S38: XPS Na 1s spectrum of substituted ferrite, $x = 0.62(1)$ point 1.
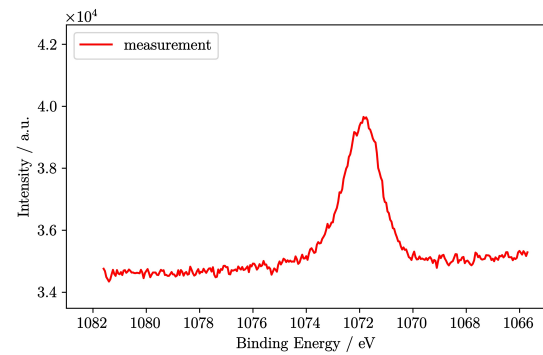
Figure S39: XPS Na 1s spectrum of substituted ferrite, $x = 0.62(1)$ point 2.
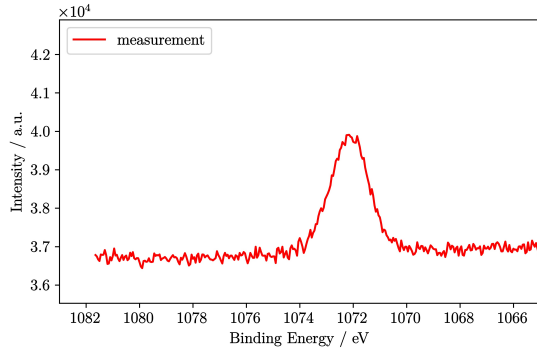
Figure S40: XPS Na 1s spectrum of substituted ferrite, $x = 0.91(7)$ point 1.
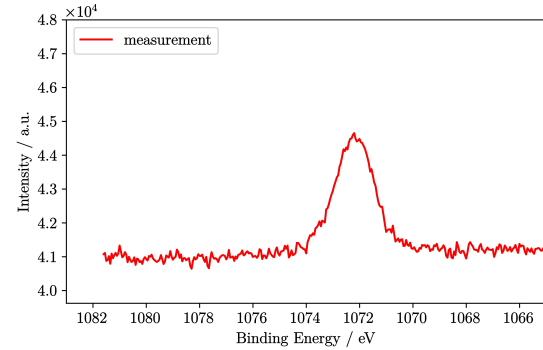
Figure S41: XPS Na 1s spectrum of substituted ferrite, $x = 0.91(7)$ point 2.
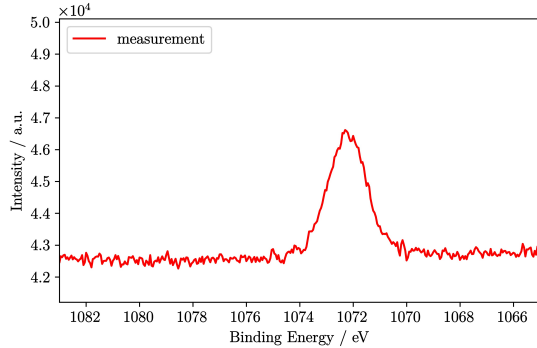
Figure S42: XPS Na 1s spectrum of substituted ferrite, $x = 0.91(7)$ point 3.
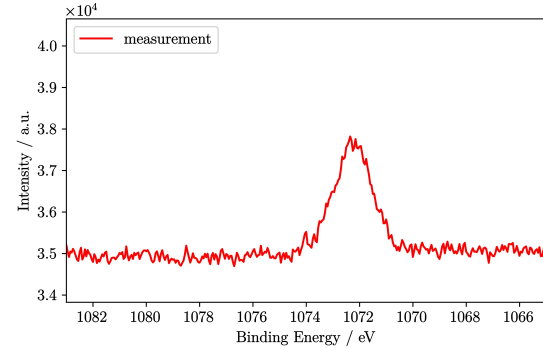
Figure S43: XPS Na 1s spectrum of substituted ferrite, $x = 0.91(7)$ point 4.
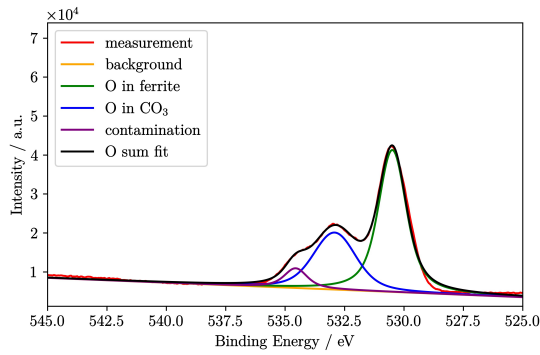
Figure S44: XPS O 1s spectrum of unsubstituted ferrite point 1.
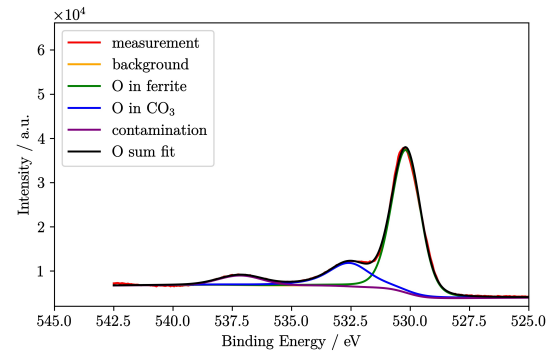
Figure S45: XPS O 1s spectrum of unsubstituted ferrite point 2.
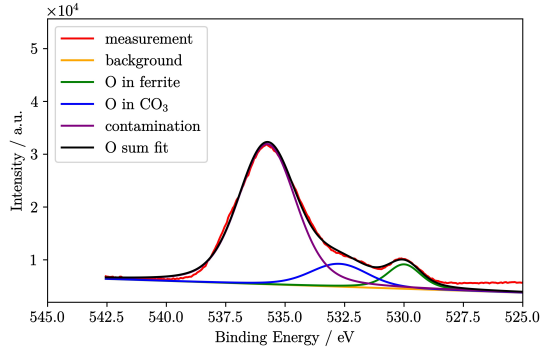
Figure S46: XPS O 1s spectrum of substituted ferrite, $x = 0.143(5)$ point 1.
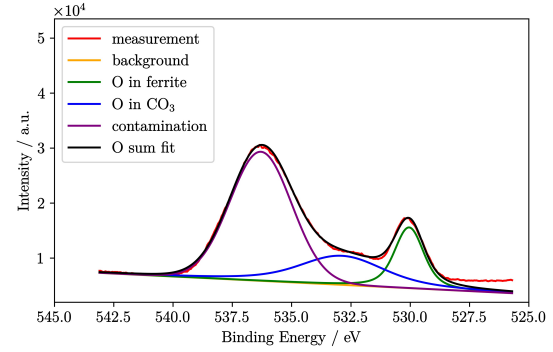
Figure S47: XPS O 1s spectrum of substituted ferrite, $x = 0.143(5)$ point 2.
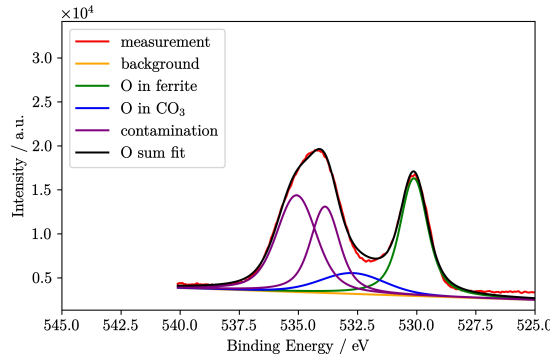

Figure S48: XPS O 1s spectrum of substituted ferrite, $x = 0.49(1)$ point 1.

Figure S49: XPS O 1s spectrum of substituted ferrite, $x = 0.62(1)$ point 1.
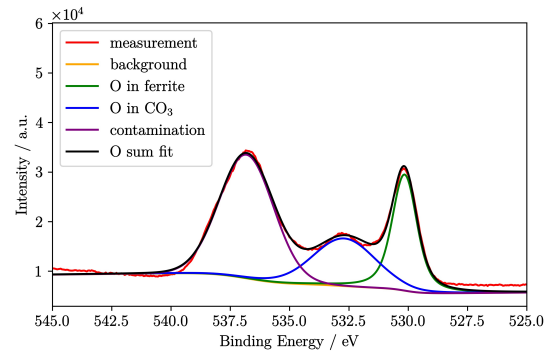
Figure S50: XPS O 1s spectrum of substituted ferrite, $x = 0.62(1)$ point 2.
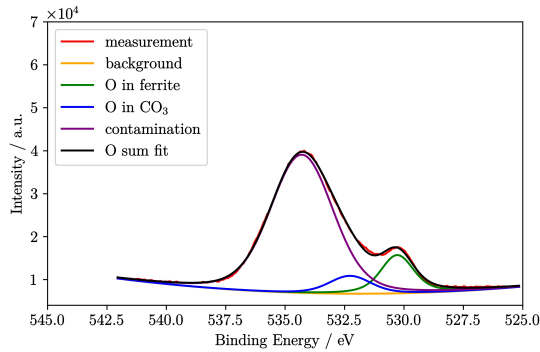
Figure S51: XPS O 1s spectrum of substituted ferrite, $x = 0.91(7)$ point 1.
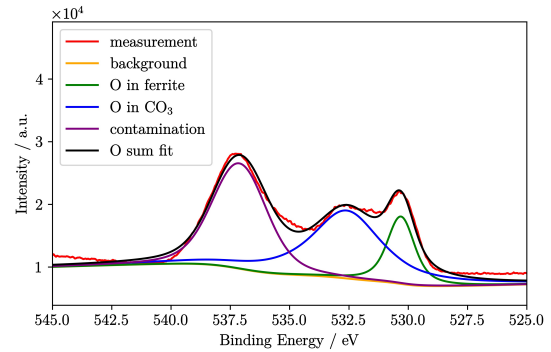
Figure S52: XPS O 1s spectrum of substituted ferrite, $x = 0.91(7)$ point 2.
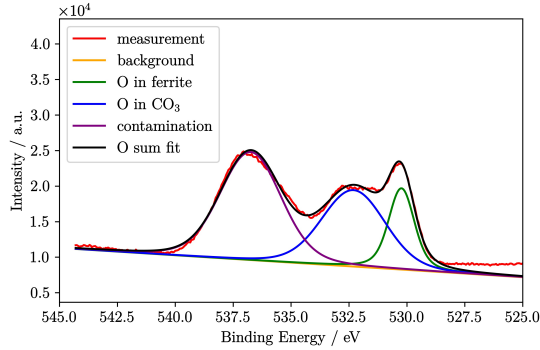
Figure S53: XPS O 1s spectrum of substituted ferrite, $x = 0.91(7)$ point 3.
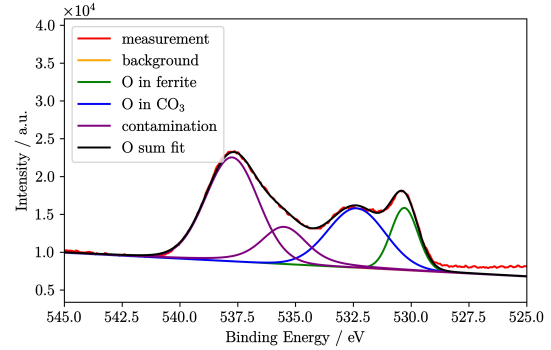
Figure S54: XPS O 1s spectrum of substituted ferrite, $x = 0.91(7)$ point 4.
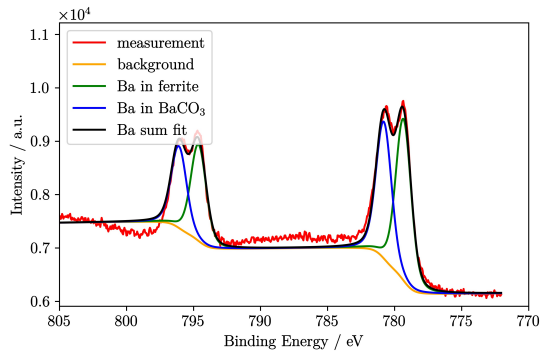
Figure S55: XPS Ba 3d spectrum of un-substituted ferrite point 1.
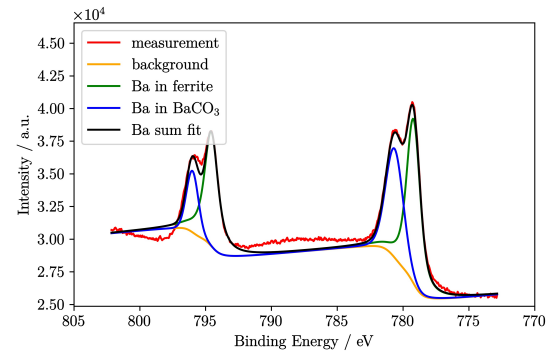
Figure S56: XPS Ba 3d spectrum of un-substituted ferrite point 2.
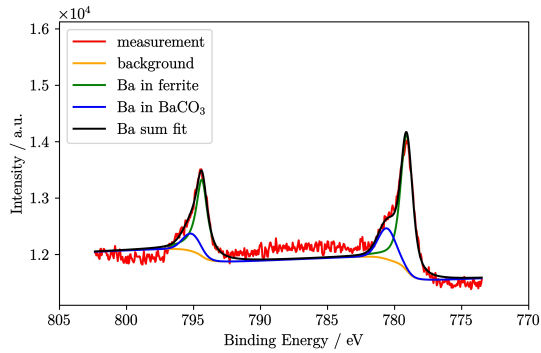
Figure S57: XPS Ba 3d spectrum of sub-stituted ferrite, $x = 0.143(5)$ point 1.
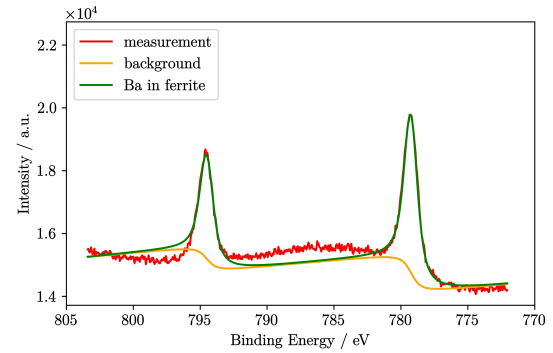
Figure S58: XPS Ba 3d spectrum of sub-stituted ferrite, $x = 0.143(5)$ point 2.
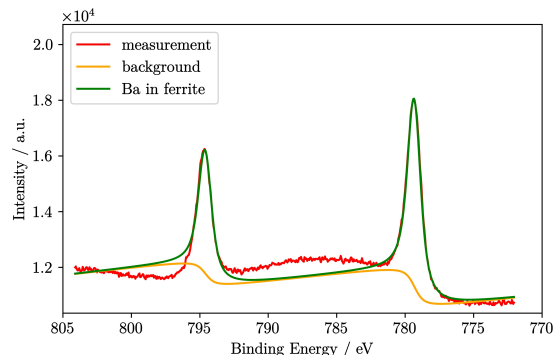
Figure S59: XPS Ba 3d spectrum of substituted ferrite, $x = 0.49(1)$ point 1.

4 XPS data
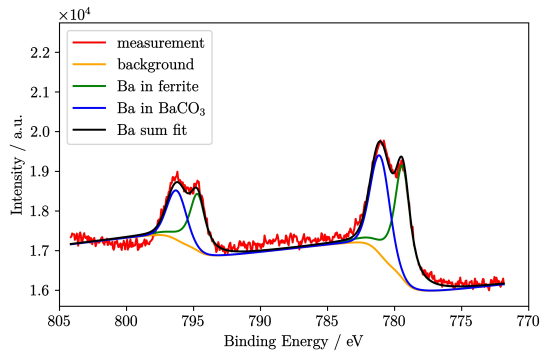
Figure S60: XPS Ba 3d spectrum of substituted ferrite, $x = 0.62(1)$ point 1.
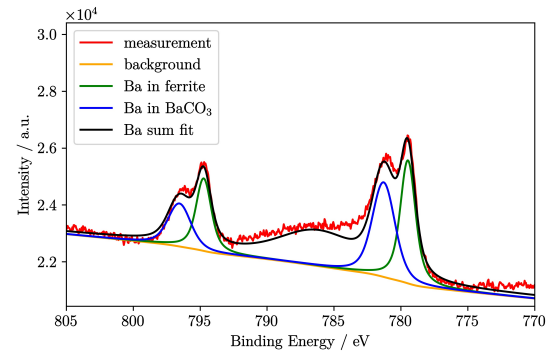
Figure S61: XPS Ba 3d spectrum of substituted ferrite, $x = 0.62(1)$ point 2.
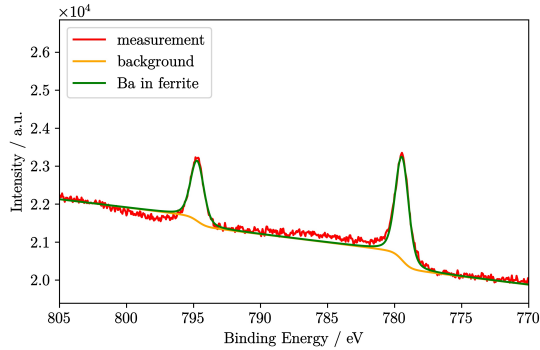
Figure S62: XPS Ba 3d spectrum of substituted ferrite, $x = 0.91(7)$ point 1.
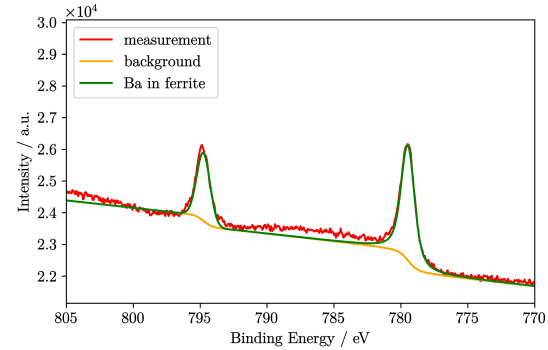
Figure S63: XPS Ba 3d spectrum of substituted ferrite, $x = 0.91(7)$ point 2.
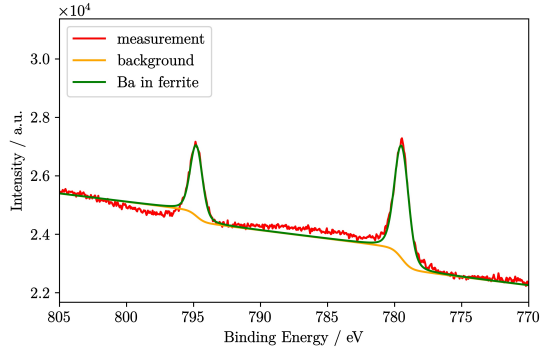
Figure S64: XPS Ba 3d spectrum of substituted ferrite, $x = 0.91(7)$ point 3.
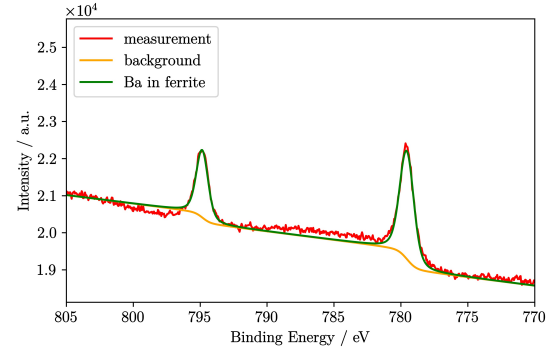

Figure S65: XPS Ba 3d spectrum of substituted ferrite, $x = 0.91(7)$ point 4.
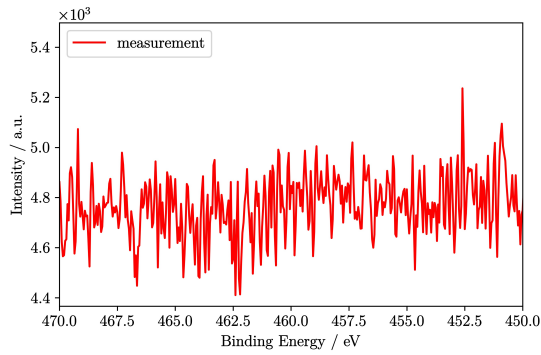
Figure S66: XPS Ti 2p spectrum of un-substituted ferrite point 1.
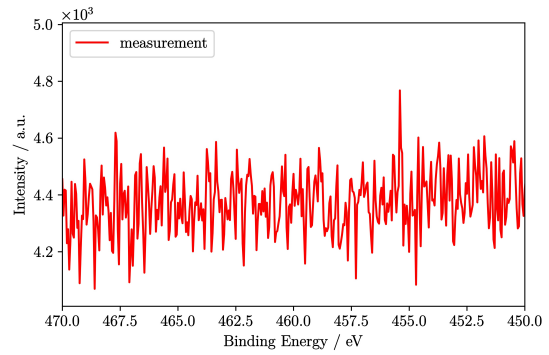
Figure S67: XPS Ti 2p spectrum of un-substituted ferrite point 2.
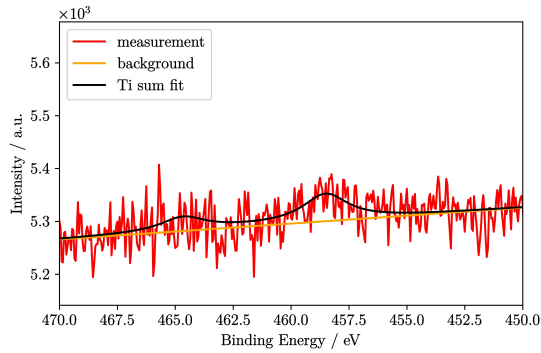

Figure S68: XPS Ti 2p spectrum of substituted ferrite, $x = 0.143(5)$ point 1.
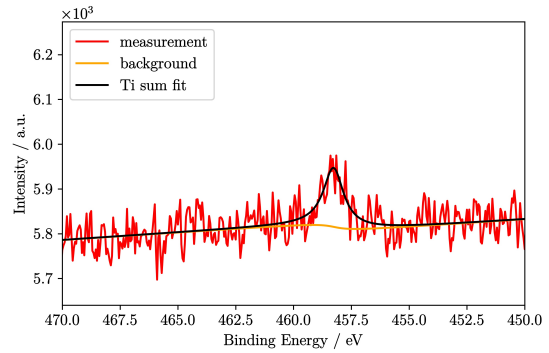
Figure S69: XPS Ti 2p spectrum of substituted ferrite, $x = 0.143(5)$ point 2.
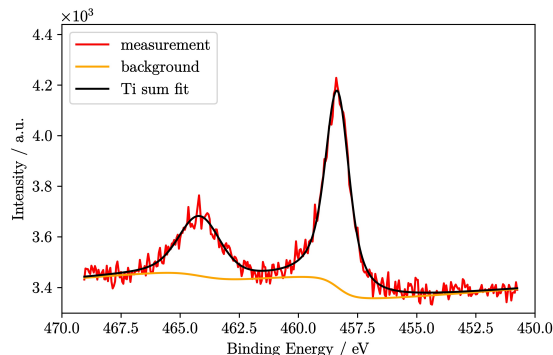
Figure S70: XPS Ti 2p spectrum of substituted ferrite, $x = 0.49(1)$ point 1.

Figure S71: XPS Ti 2p spectrum of substituted ferrite, $x = 0.62(1)$ point 1.
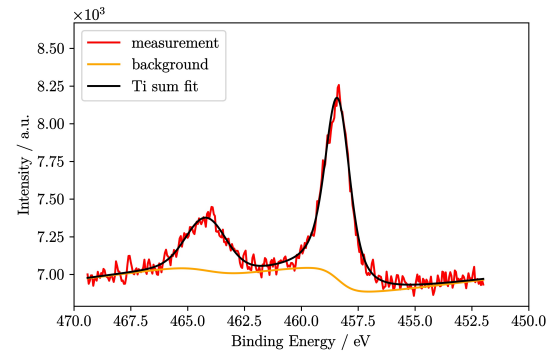
Figure S72: XPS Ti 2p spectrum of substituted ferrite, $x = 0.62(1)$ point 2.
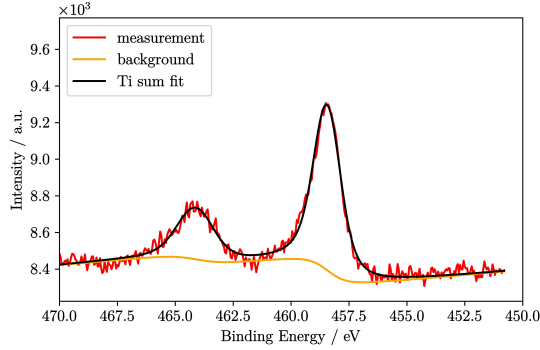
Figure S73: XPS Ti 2p spectrum of substituted ferrite, $x = 0.91(7)$ point 1.
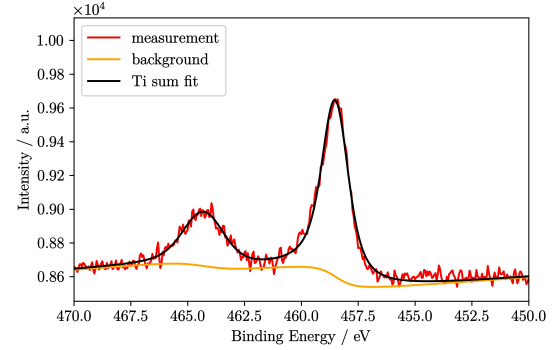
Figure S74: XPS Ti 2p spectrum of substituted ferrite, $x = 0.91(7)$ point 2.
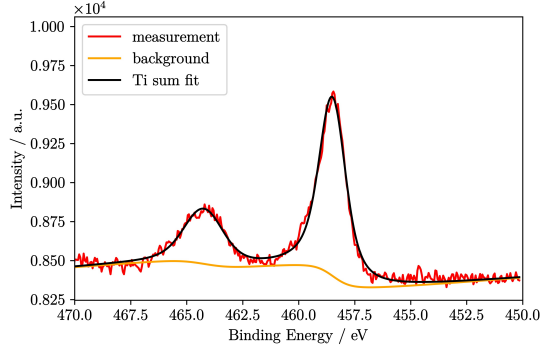
Figure S75: XPS Ti 2p spectrum of substituted ferrite, $x = 0.91(7)$ point 3.
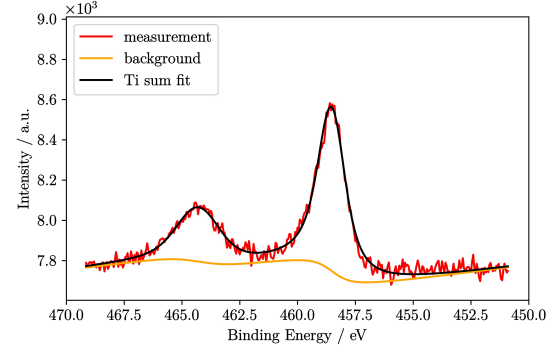
Figure S76: XPS Ti 2p spectrum of substituted ferrite, $x = 0.91(7)$ point 4.
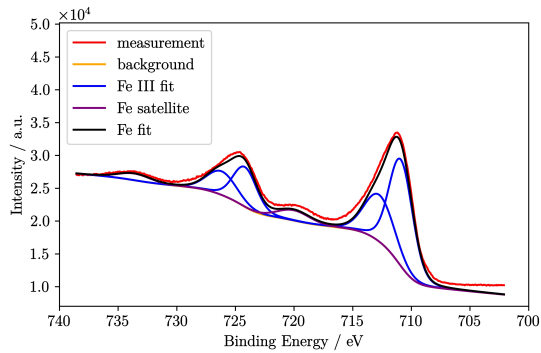
Figure S77: XPS Fe 2p spectrum of un-substituted ferrite point 1.
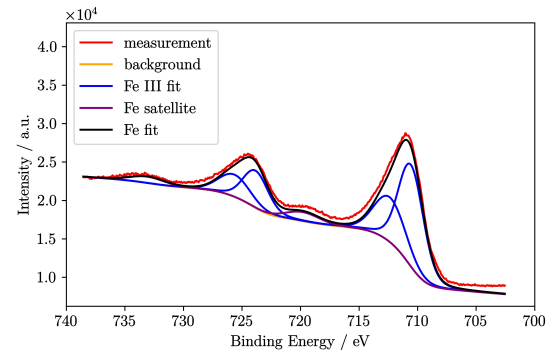
Figure S78: XPS Fe 2p spectrum of un-substituted ferrite point 2.
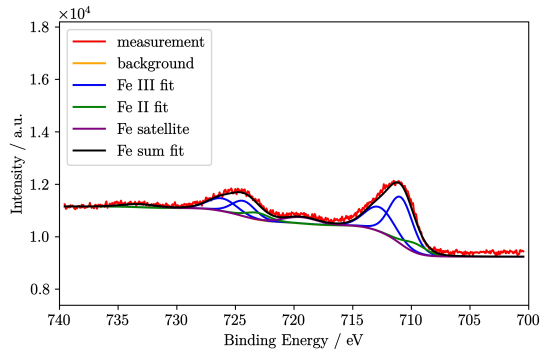
Figure S79: XPS Fe 2p spectrum of sub-stituted ferrite, $x = 0.143(5)$ point 1.
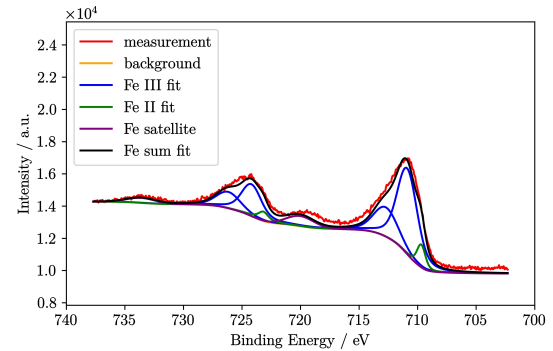
Figure S80: XPS Fe 2p spectrum of sub-stituted ferrite, $x = 0.143(5)$ point 2.
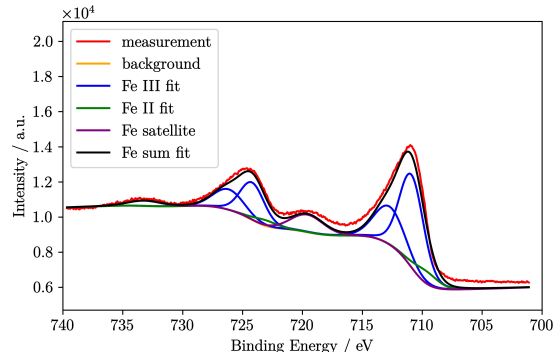
Figure S81: XPS Fe 2p spectrum of substituted ferrite, $x = 0.49(1)$ point 1.

Figure S82: XPS Fe 2p spectrum of substituted ferrite, $x = 0.62(1)$ point 1.
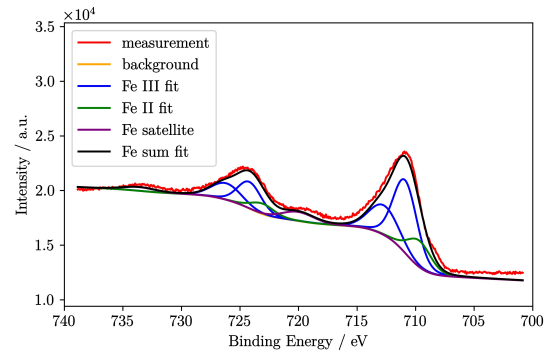
Figure S83: XPS Fe 2p spectrum of substituted ferrite, $x = 0.62(1)$ point 2.
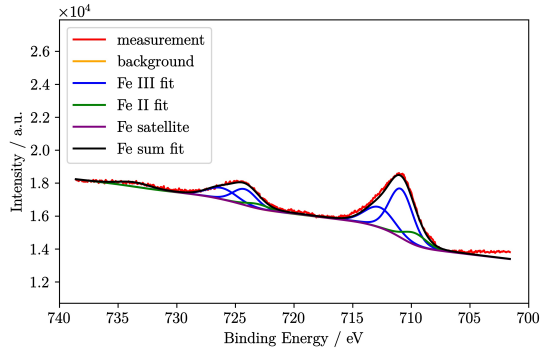
Figure S84: XPS Fe 2p spectrum of substituted ferrite, $x = 0.91(7)$ point 1
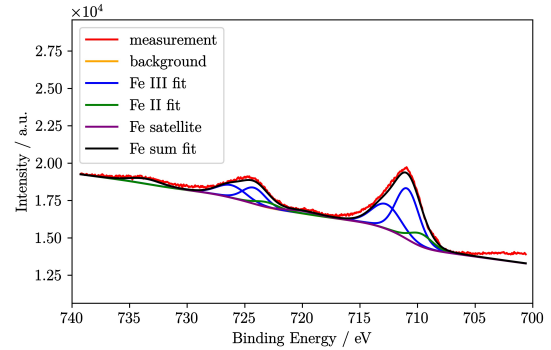

Figure S85: XPS Fe 2p spectrum of substituted ferrite, $x = 0.91(7)$ point 2.
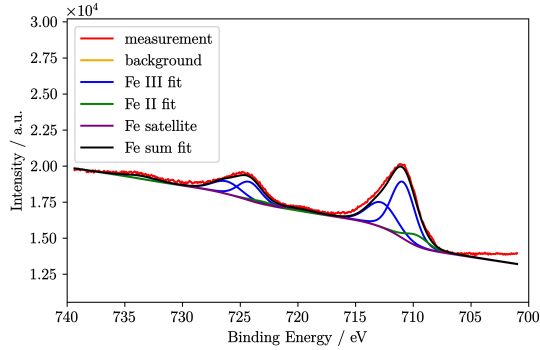

Figure S86: XPS Fe 2p spectrum of substituted ferrite, $x = 0.91(7)$ point 3.
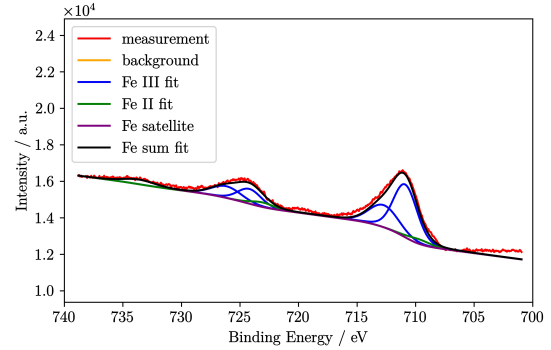
Figure S87: XPS Fe 2p spectrum of substituted ferrite, $x = 0.91(7)$ point 4.

## 4.3 XPS measurement spectra with pass energy 20 eV
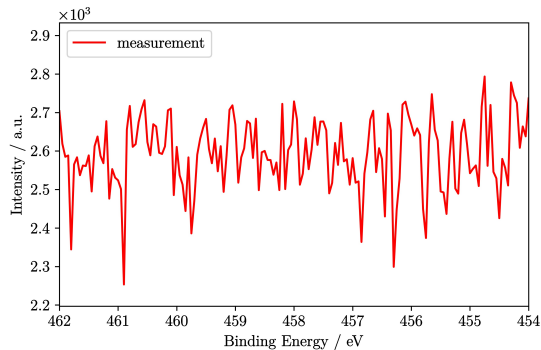
Figure S88: XPS Ti 2p spectrum of un-substituted ferrite point 1.
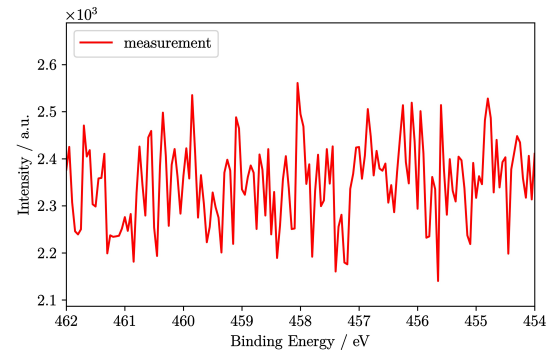
Figure S89: XPS Ti 2p spectrum of un-substituted ferrite point 2.
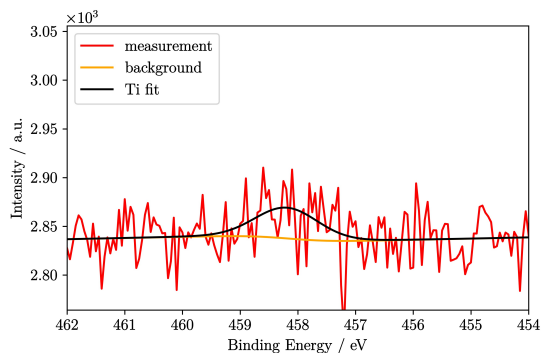
Figure S90: XPS Ti 2p spectrum of sub-stituted ferrite, $x = 0.143(5)$ point 1.
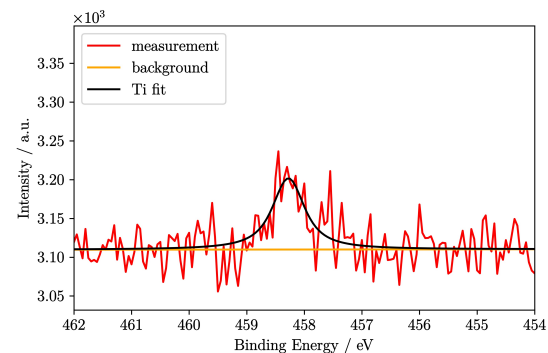
Figure S91: XPS Ti 2p spectrum of sub-stituted ferrite, $x = 0.143(5)$ point 2.
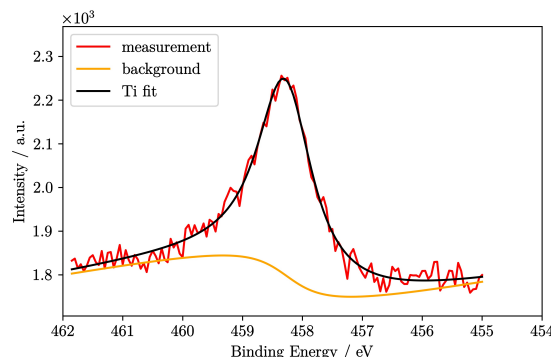
Figure S92: XPS Ti 2p spectrum of substituted ferrite, $x = 0.49(1)$ point 1.
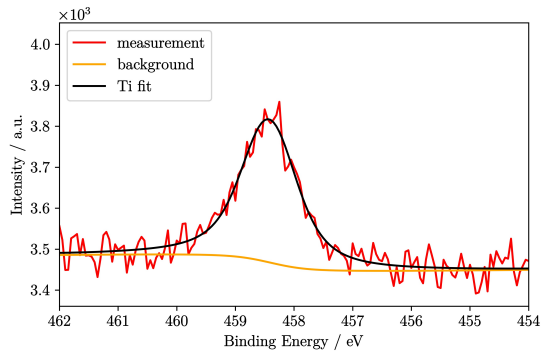
Figure S93: XPS Ti 2p spectrum of substituted ferrite, $x = 0.62(1)$ point 1.
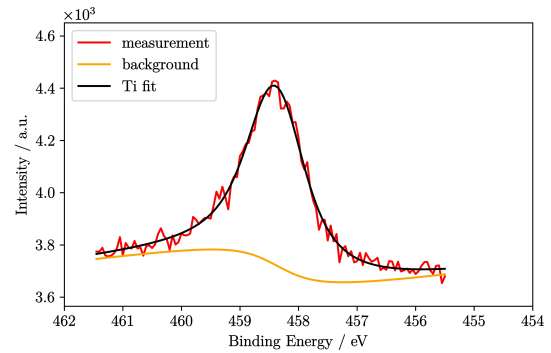
Figure S94: XPS Ti 2p spectrum of substituted ferrite, $x = 0.62(1)$ point 2.
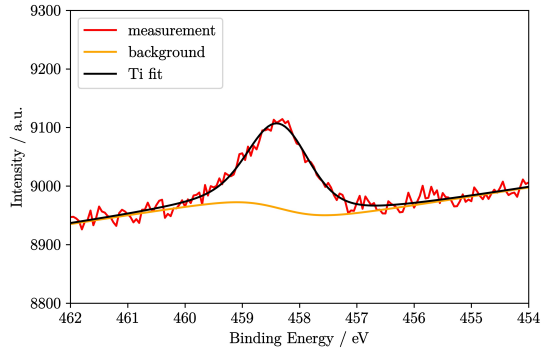
Figure S95: XPS Ti 2p spectrum of substituted ferrite, $x = 0.91(7)$ point 1.
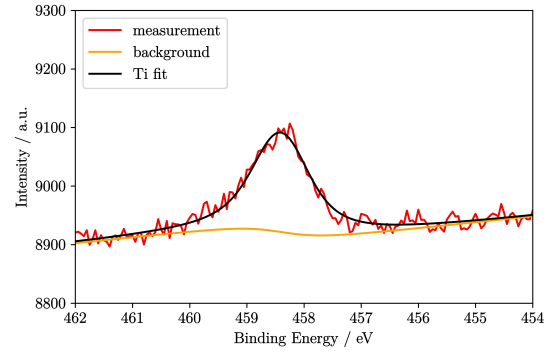
Figure S96: XPS Ti 2p spectrum of substituted ferrite, $x = 0.91(7)$ point 2.
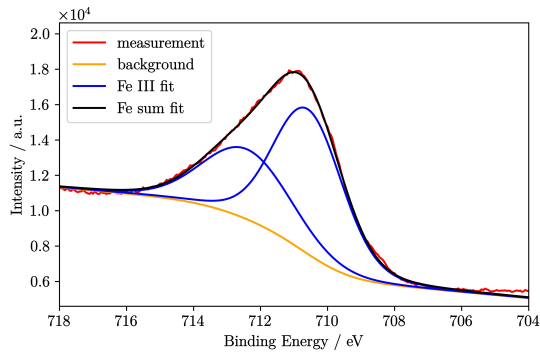
Figure S97: XPS Fe 2p spectrum of sample *a* point 1.
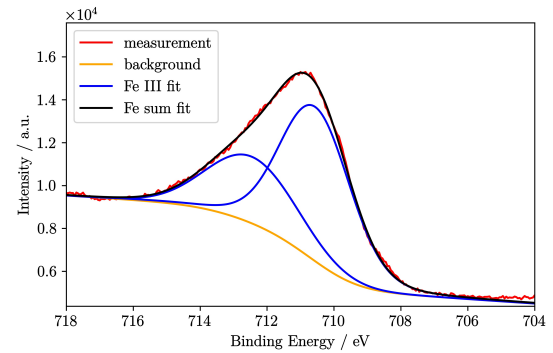
Figure S98: XPS Fe 2p spectrum of sample *a* point 2.
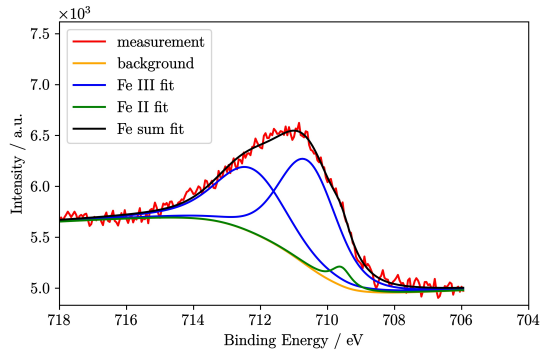
Figure S99: XPS Fe 2p spectrum of substituted ferrite, $x = 0.143(5)$ point 1.
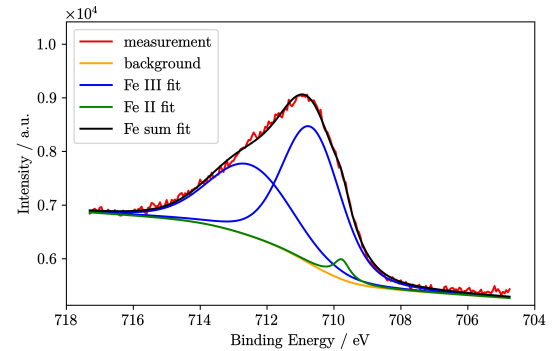
Figure S100: XPS Fe 2p spectrum of substituted ferrite, $x = 0.143(5)$ point 2.
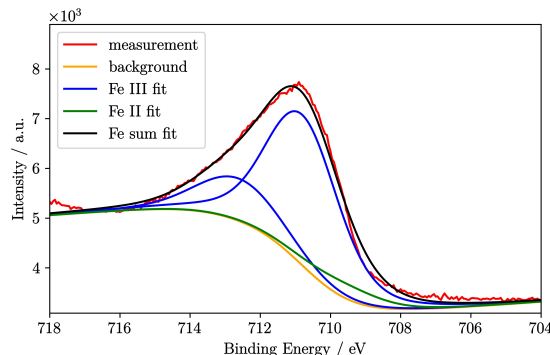
Figure S101: XPS Fe 2p spectrum of substituted ferrite, $x = 0.49(1)$ point 1.
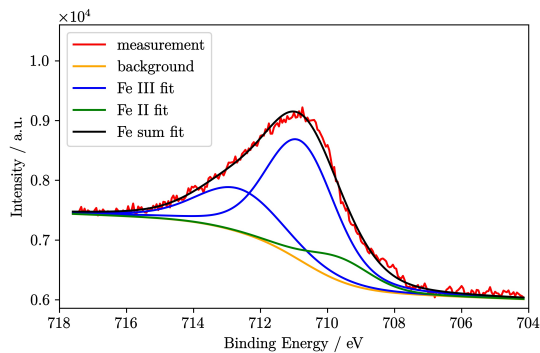
Figure S102: XPS Fe 2p spectrum of sub-
stituted ferrite, $x = 0.62(1)$
point 1.
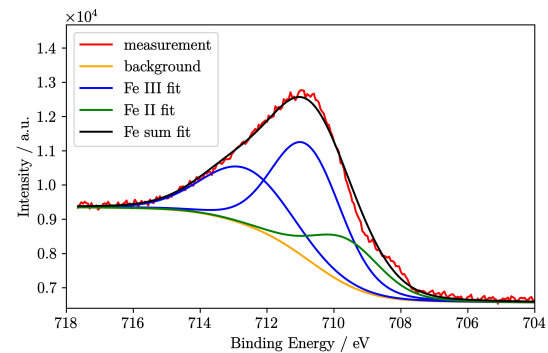
Figure S103: XPS Fe 2p spectrum of sub-
stituted ferrite, $x = 0.62(1)$
point 2.
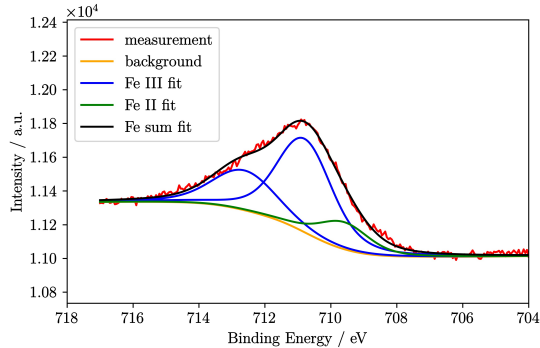
Figure S104: XPS Fe 2p spectrum of sub-
stituted ferrite, $x = 0.91(7)$
point 1.
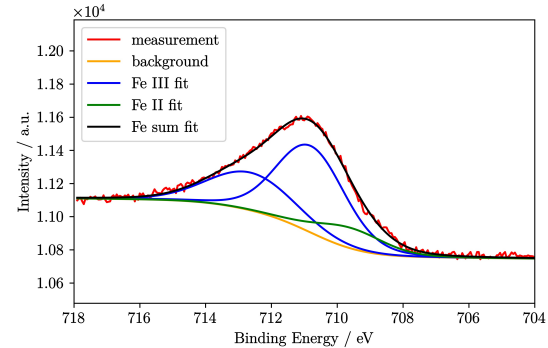
Figure S105: XPS Fe 2p spectrum of sub-
stituted ferrite, $x = 0.91(7)$
point 2.

4.4 Tables for the ratios of Fe(III), Fe(II) and/or Ti(IV) calculated from XPS measurement results

Table S16: Ratio of Fe(III)/Fe(II) in % with standard deviation in brackets determined
by XPS measurements with pass energy 20 eV.

Sample	point 1	point 2	mean
a	100/0	100/0	100/0
b	96(8)/4(8)	97(6)/3(6)	97(7)/3(7)
c	93(1)/7(1)	-	93(1)/7(1)
d	89(3)/11(3)	80(2)/20(2)	85(3)/15(3)
e	85(4)/15(4)	87(4)/13(4)	86(4)/14(4)

4 XPS data

Table S17: Ratio of Fe(III)/Fe(II) in % with standard deviation in brackets determined by XPS measurements with pass energy 30 eV.

Sample	point 1	point 2	point 3	point 4	mean
a	100/0	100/0	-	-	100/0
b	87(23)/12(23)	92(16)/8(16)	-	-	90(25)/10(25)
c	92(1)/8(1)	-	-	-	92(1)/8(1)
d	84(1)/16(1)	78(36)/22(36)	-	-	81(19)/19(19)
e	87(1)/13(1)	86(1)/14(1)	90(1)/10(1)	92(1)/8(1)	89(1)/11(1)

Table S18: Ratio of Fe(II)/Ti(IV) in % with standard deviation in brackets determined by XPS measurements with pass energy 20 eV.

Sample	point 1	point 2	mean
a	0/0	0/0	0/0
b	65(23)/35(23)	-	65(23)/35(23)
c	35(1)/65(1)	-	35(1)/65(1)
d	46(5)/54(5)	58(1)/42(1)	52(3)/48(3)
e	40(31)/60(31)	35(22)/65(22)	38(27)/62(27)

Table S19: Ratio of Fe(II)/Ti(IV) in % with standard deviation in brackets determined by XPS measurements with pass energy 30 eV.

Sample	point 1	point 2	point 3	point 4	mean
a	0/0	0/0	-	-	0/0
b	72(20)/28(20)	78(17)/22(17)	-	-	75(19)/25(19)
c	39(13)/61(13)	-	-	-	39(13)/61(13)
d	51(24)/49(24)	59(31)/41(31)	-	-	55(28)/45(28)
e	34(9)/66(9)	33(7)/67(7)	26(6)/74(6)	20(7)/80(7)	28(7)/72(7)

Table S20: Ratio of Fe(III)/Fe(II)/Ti(IV) in % with standard deviation in brackets determined by XPS measurements with pass energy 20 eV.

Sample	point 1	point 2	mean
a	100/0 / 0	100/0/0	100/0/0
b	94(10)/4(8)/2(2)	-	94(10)/4(8)/2(2)
c	82(7)/6(1)/12(7)	-	82(7)/6(1)/12(7)
d	79(13)/10(4)/11(12)	70(7)/17(3)/12(7)	75(10)/13(4)/12(10)
e	69(18)/13(6)/18(19)	69(15)/11(4)/20(15)	69(17)/12(5)/19(17)

4 XPS data

Table S21: Ratio of Fe(III)/Fe(II)/Ti(IV) in % with standard deviation in brackets determined by XPS measurements with pass energy 30 eV.

Sample	point 1	point 2	point 3	point 4	mean
a	100/0/0	100/0/0	-	-	100/0/0
b	83(24)/12(21)/5(5)	89(17)/8(15)/3(2)	-	-	86(21)/10(18)/4(4)
c	82(5)/7(1)/11(5)	-	-	-	82(5)/7(1)/11(5)
d	73(10)/14(2)/13(11)	68(40)/19(30)/13(16)	-	-	71(25)/16(16)/13(14)
e	68(6)/11(1)/21(6)	68(5)/11(1)/21(5)	70(5)/8(1)/22(5)	71(8)/6(1)/23(8)	69(6)/9(1)/22(6)